Drug Design, Development and Therapy

Dovepress
open access to scientific and medical research

Open Access Full Text Article

ORIGINAL RESEARCH

Metabolomics Study of Shaoyao Plants Decoction on the Proximal and Distal Colon in Mice with Dextran Sulfate Sodium-Induced Colitis by UPLC-Q-TOF-MS

Yiting Luo[1], Jin Wu[1], Yingchao Liu[2], Yan Shen[3], Fangyuan Zhu[1], Jiaqian Wu[1], Yuyao Hu[3]

[1]The Second Clinical Medical College, Zhejiang Chinese Medical University, Hangzhou, People's Republic of China; [2]Academic Affairs Office, Zhejiang Chinese Medical University, Hangzhou, People's Republic of China; [3]The Second Affiliated Hospital of Zhejiang Chinese Medical University, Hangzhou, People's Republic of China

Correspondence: Yuyao Hu, The Second Affiliated Hospital of Zhejiang Chinese Medical University, 318 Chaowang Road, Hangzhou, People's Republic of China, Email 20094017@zcmu.edu.cn

Purpose: Shaoyao decoction (SYD) is a traditional Chinese medicine used to treat ulcerative colitis (UC). The exact mechanism of action of SYD in UC treatment is still unclear. Here, we examined the therapeutic effects of SYD in mice with dextran sulfate sodium (DSS)-induced colitis and explored the underlying mechanism.

Methods: The experimental group was divided into normal control, UC, and SYD treatment groups. The UC model of C57BL/6 mice was induced using 3% (w/v) DSS for 7 days. SYD was orally administered for 7 days. The proximal and distal colonic metabolic profiles were detected using quadrupole-time-of-flight mass spectrometry-based untargeted metabolomics.

Results: SYD significantly increased weight, reduced disease activity index scores, and ameliorated colon length shortening and pathological damage in mice. In the distal colon, SYD increased the abundance of phosphatidic acid and lysophosphatidylethanolamine and decreased the abundance of lactosylceramide, erythrodiol 3-palmitate, and lysophosphatidylcholine. In the proximal colon, SYD increased the abundance of palmitic acid, cyclonormammein, monoacylglyceride, 13S-hydroxyoctadecadienoic acid, and ceanothine C and decreased the abundance of tetracosahexaenoic acid, phosphatidylserine, and diglyceride.

Conclusion: Our findings revealed that SYD could alleviate UC by regulating metabolic dysfunction, which provides a reference for further studies on SYD.

Keywords: Shaoyao decoction, ulcerative colitis, metabolomics, UPLC-Q-TOF-MS, DSS-induced colitis mouse model

Introduction

Ulcerative colitis (UC), a major inflammatory bowel disease (IBD),[1] is characterized by mucosal epithelial damage and disruption of intestinal homeostasis and manifests as abdominal pain, diarrhea, and bloody mucus in stools.[2–4] The etiology of UC is complex and includes genetic susceptibility, defective immune responses, and environmental factors'.[5,6] The morbidity rate of IBD is 5–15 per 100,000 persons per year in the Western world, and the incidence of UC is increasing in both developed and developing countries'.[7–11] Currently, the different drugs used to treat UC include aminosalicylates, steroids, immunosuppressants, and biological agents.[12,13] Although these drugs are generally effective, not all patients respond to or achieve sustained remission, and their use has certain limitations, such as an increased risk of infection and malignancy.[14–16] The disadvantages of the current therapies make the prospect of using traditional Chinese medicine to treat UC even more appealing.

Traditional Chinese medicine is a multicomponent, multichannel, and multitarget therapeutic drug widely used in China and has a long history. It has shown great advantages in treating and preventing diseases and has accumulated rich experience.[17,18] Shaoyao decoction (SYD) is a traditional herbal medicine composed of Baishao, Danggui, Huanglian,

Received: 15 September 2022
Accepted: 9 December 2022
Published: 22 December 2022

Huangqin, Gancao, Binglang, Muxiang, Dahuang, and Rougui. SYD has multiple pharmacological activities and is widely used for the treatment of UC. Baishao has anti-inflammatory and antioxidant properties.[19] Danggui has anti-inflammatory and anti-cancer effects.[20] Berberine, a major component of Huanglian, acts on many organs and systems of the body and has many biological functions, such as anti-inflammatory, anti-tumor, anti-arrhythmic, and blood lipid regulation.[21–23] Huangqin has a variety of biological activities, including antioxidant, antiviral, antibacterial, anti-inflammatory, and anti-tumor functions.[24] Many clinical studies have shown that SYD has a therapeutic effect on UC.[25–28] In addition to the clinical efficacy of SYD, some studies have reported mechanisms of SYD in the treatment of UC. In a dextran sulfate sodium (DSS)-induced colitis mouse model, Chi et al found that SYD could regulate the signal pathway of STAT3 and NF-κB and regulate epithelial cell apoptosis and permeability.[29] Wei et al demonstrated that SYD alleviates pyroptosis by regulating the MKP1/NF-κB/NLRP3 pathway.[30] Moreover, SYD may regulate the abundance and changes in the gut microbiota and play a role in the treatment of UC.[31] Although some studies have reported these mechanisms, the pathogenesis of UC is complex, and the mechanism of SYD in the treatment of UC needs to be further clarified.

In recent years, metabolites produced by the intestinal flora have been shown to play a key role in regulating intestinal mucosal homeostasis. These metabolites are produced and secreted into the lumen and regulate the activity of many host cell types, including immune and intestinal epithelial cells.[32–35] These metabolites, including short-chain fatty acids (SCFAs) and lipids, can influence the health and disease state of hosts.[36] Studies have found that the content of SCFAs in patients with UC decreased.[37,38] SCFAs can repair intestinal epithelial cells, promote the production of mucin by goblet cells, modify tight junction proteins, and improve the integrity of the intestinal mucosal barrier.[39–41] In addition, studies have found that UC is associated with alterations in lipid metabolism.[42,43] Lipids control cellular processes, such as proliferation, differentiation, migration, and apoptosis.[44,45] Currently, most studies have focused on changes in metabolites in feces, plasma, and urine, and few studies have examined metabolic changes in the colon tissue. However, research showed that the intestinal mucosa absorbs 90–95% of SCFAs produced by the gut microbiota, and SCFAs have the highest concentration in colon tissue.[46–49] Therefore, the study of changes in intestinal metabolites in UC should not be limited to feces but should focus on the colon tissue.

Metabolomics is a technology for the qualitative and quantitative analysis of metabolites in a given organism or biological sample, which can detect small molecular substances and precisely display the changes that occur in the body.[50,51] Presently, the commonly used techniques in metabolomics include nuclear magnetic resonance (NMR), gas chromatography-mass spectrometry (GC-MS), and ultra-performance liquid chromatography combined with quadrupole-time-of-flight mass spectrometry (UPLC-Q-TOF-MS). UPLC-Q-TOF-MS is a powerful metabolomics technology owing to its high resolution and sensitivity.[52] In addition, non-targeted analysis has a wide application in drug research by probing biomarkers to clarify the underlying mechanisms of drugs.[53] In recent years, the widespread use of this technology has provided a new perspective for traditional Chinese medicine research.[54–56]

This study aimed to explore the effects of SYD on colon metabolites in a murine model of DSS-induced UC. UPLC-Q-TOF-MS-based untargeted metabolomics was used to analyze the changes in colon metabolites. At the same time, we also compared the differences in the proximal and distal colonic metabolic profiles to provide more precise evidence for SYD in the treatment of UC. Our study provides a new perspective for further elucidation of the mechanism of SYD in the treatment of UC.

Materials and Methods

Chemicals and Reagents

Dextran sulfate sodium (DSS) (M. W.:36,000–50,000) was purchased from MP Biomedicals Corporation (Santa Ana, CA, USA), methanol and acetonitrile were purchased from EMD Millipore Corporation (Darmstadt, Germany), and formic acid was purchased from Shanghai Aladdin Biochemical Technology Limited Liability Company (Shanghai, China).

Table 1 Composition Information of Each Chinese Herbal Medicine in SYD

Chinese Name	Latin Name	The Adult Daily Dose of Herb (g)	Composition Ratio (%)
Shaoyao	Paeoniae Radix Alba (Paeonia lactiflora Pall.)	30	28.0%
Danggui	Angelicae Sinensis Radix (Angelica sinensis (Oliv.) Diels)	15	14.0%
Huanglian	Coptidis Rhizoma (Coptis chinensis Franch.)	15	14.0%
Huangqin	Scutellariae Radix (Scutellaria baicalensis Georgi)	15	14.0%
Dahuang	Rhei Radix et Rhizoma (Rheum palmatum L., R. tanguticum Maxim. ex Balf. or R. officinale Bail)	9	8.5%
Binglang	Arecae Semen (Areca catechu L.)	6	5.6%
Muxiang	Aucklandiae Radix (Aucklandia costus Falc.)	6	5.6%
Gancao	Glycyrrhizae Radix et Rhizoma (Glycyrrhiza uralensis Fisch., Glycyrrhiza inflata Bat. or Glycyrrhiza glabra L.)	6	5.6%
Rougui	Cinnamomi Cortex (Cinnamomum verum J. Presl)	5	4.7%

Preparation of SYD

SYD comprises nine different herbs, including Baishao, Danggui, Huanglian, Huangqin, Gancao, Binglang, Muxiang, Dahuang, and Rougui. Details of their composition are shown in Table 1. All herbs were purchased from the Second Affiliated Hospital of Zhejiang Chinese Medical University (Hangzhou, Zhejiang, China) and accredited by a pharmacologist. The dose of SYD for experimental mice was determined according to the clinical equivalent dosage and study by Chi et al.[29] The daily clinical dose of SYD in humans is 107 g. According to the formula of equivalent body surface area between humans and mice,[57] the dose for a mouse is 17.8 g/kg/day. All raw herbs were soaked in distilled water (1:10, w/v) for 30 min, boiled for 1 h, filtered with gauze, filtrate collected, decocted the residue with distilled water (1:6, w/v) as described above, combined the two filtrates, and concentrated them to 1 g/mL using a rotary evaporator at 60°C. Part of the SYD liquid was stored at −80°C for UPLC-QTOF-MS analysis (Waters Corporation, Ireland).

UPLC-Q-TOF-MS Analysis for SYD

The liquid SYD was thawed at 4°C, diluted with methanol to 100 mg/mL, the mixture was stirred and ultrasonicated for 15 min, and centrifuged at 12,000 x *g* for 10 min. The supernatant was obtained for UHPLC-Q-TOF-MS analysis (Waters Corporation, Ireland). The SYD liquids were analyzed in negative and positive modes on the ACQUITY UPLC HSS T3 column (100 mm × 2.1 mm, 1.8 μm; Waters Corporation, Ireland) at a flow rate of 0.3 mL/min, sample injection volume of 2.0 μL, autosampler temperature of 4°C and column temperature of 40°C. Mobile phases A and B were 0.1% (v/v) formic acid/water and 0.1% (v/v) formic acid/acetonitrile, respectively. The gradient elution conditions were set as follows: 20% B for 0–2 min, 52% B for 12 min, 65% B for 18 min, 90% B for 22 min, and 20% B for 26–30 min. The mass spectrum parameters of the positive mode were capillary voltages: 3.0 kV, sampling cone: 40.0 V, source temperature: 100°C, desolvation temperature: 500°C, cone gas flow: 100°C, desolvation gas flow: 1000.0 L/h, scan time: 0.10 s, interscan time: 0.014 s, mass range: 50–2000 m/z. The mass spectrum parameters of the negative mode were capillary voltages: 2.5 kV, sampling cone: 40.0 V, source temperature: 100°C, desolvation temperature: 500°C, cone gas flow: 100°C, desolvation gas flow: 1000.0 L/h, scan time: 0.10 s, interscan time: 0.014 s, mass range: 50–2000 m/z.

Animals

Forty male C57BL/6 mice (6–8 weeks old, 20–22 g) were purchased from the Shanghai Slack Laboratory Animal Limited Liability Company (No. SCXK 2017–0005). All mice were housed under standard laboratory conditions (55 ± 10% humidity, 22 ± 2°C, and 12 h light/dark cycle). Animal welfare was performed according to the guidelines for the management and use of laboratory animals (Ministry of Science and Technology, China, 2016). The experimental protocol was approved by the Experimental Animal Ethics Committee of the Zhejiang Chinese Medical University (IACUC-20210531-02).

Animal Model Establishment and Treatment Procedures

After the seven days of acclimatization, 40 C57BL/6 mice were randomly divided into three groups: the normal control (NC) group (n = 10), UC model (UC) group (n = 15), and SYD treatment (SYD) group (n = 15). To establish the UC model, the mice in the UC and SYD groups received drinking water containing 3% (w/v) DSS for seven days,[58] whereas those in the NC group were given distilled water. After the successful establishment of the murine model of UC, the mice in the SYD group were given 17.8 g/kg SYD once a day by gastric gavage for seven days,[29] and the mice in the NC and UC groups were given equal amounts of distilled water at the same time and in the same manner.

Disease Activity Index (DAI)

Body weight, stool consistency, and stool blood levels of mice were recorded daily, and the calculation of the DAI score was based on an earlier study, which was the average score of weight loss, stool consistency, and occult/gross bleeding (Table 2).[59]

Sample Collection and Preparation

After seven days of treatment, the mice were euthanized using CO2, and the lengths of the colons were photographed and measured. For colon, tissue from the ileocecal junction to the rectum was divided into two equal halves of approximately 2.5–4 cm in length representing proximal and distal colon.[60,61] The proximal colon was morphologically distinct from the remaining parts of the tissue by transverse folds that project into the lumen.[62] Then, the proximal colon and distal colon of each mouse were cut into pieces; one piece of the proximal colon and distal colon was fixed in 4% paraformaldehyde, and the remaining pieces from a colon were stored at −80 °C for subsequent use.

Histopathological Analysis

The colons fixed in 4% paraformaldehyde were embedded in paraffin, stained with hematoxylin and eosin (H&E) staining, and examined under light microscopy. Histopathological scores were calculated according to damage to the epithelial mucosa and inflammatory infiltration, as shown in Table 3.[59]

Untargeted Analysis Using UPLC-Q-TOF-MS

Preparation of Metabolomic Samples

Before analysis, the colon samples were freeze dried separately in liquid nitrogen and ground into a powder,100 mg of each sample was collected, thawed at 4°C, and aliquoted with 1 mL methanol to precipitate proteins. The mixture was stirred for 15 min, then centrifuged at 12,000 × *g* for 10 min, and the supernatant was obtained for UHPLC-Q-TOF-MS analysis. In addition, quality control (QC) samples were prepared, which were hybrids of 10 μL of each extraction mixture.[54]

UHPLC-Q-TOF-MS Conditions

All samples were analyzed in negative and positive modes on an ACQUITY UPLC HSS T3 column (100 mm × 2.1 mm, 1.8 μm; Waters Corporation, Ireland) at a flow rate of 0.3 mL/min, sample injection volume of 2.0 μL, autosampler temperature of 4°C, and column temperature of 40°C. Mobile phases A and B were 0.1% (v/v) formic acid/water and 0.1% (v/v) formic acid/

Table 2 Criteria for Disease Activity Index

Occult/Gross Bleeding	Weight Loss (%)	Stool Consistency	Score
Normal	0	Normal	0
	1–5		1
Hemoccult positive	5–10	Loose stool	2
	10–15		3
Gross bleeding	>15	Diarrhea	4

Table 3 Evaluation of Histopathological Score

Epithelial Cells	Inflammatory Cell Infiltration	Score
Normal form	No infiltration	0
Goblet cell loss	Infiltration in basal layer of crypt	1
Large area loss of goblet cells	Infiltration reaches the mucosal muscle layer	2
Crypt cells loss	Infiltration deep into the mucosal muscle layer, accompanied by mucosal thickening and edema	3
Large area loss of crypt cells	Infiltration to the submucosa	4

acetonitrile, respectively. The gradient elution conditions were set as follows: 20% B for 0–2 min, 52% B for 12 min, 65% B for 18 min, 90% B for 22 min, and 20% B for 26–30 min. The mass spectrum parameters of the positive mode were capillary voltages: 3.0 kV, sampling cone: 40.0 V, source temperature: 100°C, desolvation temperature: 500°C, cone gas flow: 86°C, desolvation gas flow: 815.0 L/h, scan time: 0.10 s, interscan time: 0.014 s, mass range: 50–2000 m/z. The mass spectrum parameters of the negative mode were capillary voltages: 2.5 kV, sampling cone: 40.0 V, source temperature: 100°C, desolvation temperature: 500°C, cone gas Flow: 100°C, desolvation gas flow: 1000.0 L/h, scan time: 0.10 s, interscan time: 0.014 s, mass range: 50–2000 m/z. Leucine enkephalin was used as the lock mass control compound (m/z 556.2771 in the positive mode, m/z 554.2615 in the negative mode). Before beginning the analysis, a blank sample was injected three times, after which a blank sample was injected eight times, and the QC sample was injected ten times. All the samples were randomly sequenced.

Untargeted Metabolomics Analyses

All data were obtained using MassLynx V4.1 software (Waters Corporation, Milford, MA, USA) and then imported into Progenesis QI V2.0 software (Waters Corporation, Milford, MA, USA) for preprocessing. The Human Metabolome Database (HMDB, http://www.HMDB.ca), Lipid Maps (http://www.lipidmaps.org), NIST (https://www.nist.gov/), and ChemSpider (http://www.chemspider.com/) were used to speculate and identify the compounds. The data stabilized as normal distributions were imported into the SIMCA-p14.1 software, and Pareto scaling was selected for multivariate statistical analysis, including principal component analysis (PCA) and orthogonal partial least squares discriminant analysis (OPLS-DA).[54] The quality of the OPLS-DA model was assessed using 10-fold cross-validation, CV-ANOVA, 200 permutation tests, and Q2 values. Differential metabolites were screened using a combination of univariate and multivariate analyses. Metabolites with variable importance in the projection (VIP) ≥ 1 in the OPLS-DA analysis and a P value less than 0.05 in two-sample t-tests were considered significantly differential metabolites between the two groups. The significantly altered metabolites were analyzed using MetaboAnalyst 5.0.[63] Finally, the Kyoto Encyclopedia of Genes and Genomes (KEGG) database was used to confirm the metabolic pathways caused by these significantly altered metabolites.[64]

Statistical Analysis

Statistical software SPSS 21.5 (IBM Corporation, USA) was used for the data analysis and processing. The data are expressed as mean ± standard deviation. The Shapiro–Wilk test was performed to assess the data distribution. The ANOVA statistical test was used to compare the data among multiple groups when the data were normally distributed, and the least significant difference post-hoc test was performed following the ANOVA statistical test. The Kruskal–Wallis test, which is a non-parametric test, was used when the data were non-normally distributed. Statistical significance was set at $P<0.05$.

Results

Analysis of the Components of SYD

UPLC-Q-TOF-MS was used to identify the major chemical components of SYD. Twelve compounds were distinguished: gallic acid, liquiritin, glycyrrhizin, arecoline, baicalin, trans-ferulic acid, chlorogenic acid, berberine, licoisoflavone A, quercetin, formononetin, and kaempferol. The ion chromatograms are shown in Figure S1. The Identification results of

the major chemical components of SYD are shown in Table S1. Three batches of SYD were tested, and the active gradients of SYD were essentially the same, indicating that the results were reliable and robust. The identification results for the other two batches of SYD are shown in Figures S2 and S3.

SYD Alleviates DSS-Induced UC in Mice

To confirm the therapeutic effect of SYD on UC, we assessed colitis in mice based on weight, DAI score, and colon length. Compared with the NC group, the weight of the mice that received DSS significantly decreased (Figure 1A). On day 7 of DSS induction, the DAI score of mice that received DSS was significantly higher than that of the mice in the NC group (Figure 1B). These results suggested that the UC mouse model was successfully established. After administration of SYD, the weight loss and DAI score improved (Figure 1A and C). Furthermore, we measured the colon length (Figure 1D) and observed a reduction of approximately 14.52% and 0.50% in the UC and SYD groups, respectively, compared with that of the NC group. The colon length of mice in the UC group was significantly shorter than those in the NC ($P<0.001$) and SYD groups ($P<0.001$). There were no differences between the NC and SYD groups (Figure 1E).

SYD Improved Mucosal Inflammation of Colonic Tissues

Typical histopathological manifestations in the proximal colon and distal colon of mice in each group are shown in Figure 2A and B. The colons of mice in the NC group showed complete colonic epithelium and no inflammatory cell infiltration. In the UC group, the colons of mice showed high levels of inflammatory cell infiltration in the intestinal

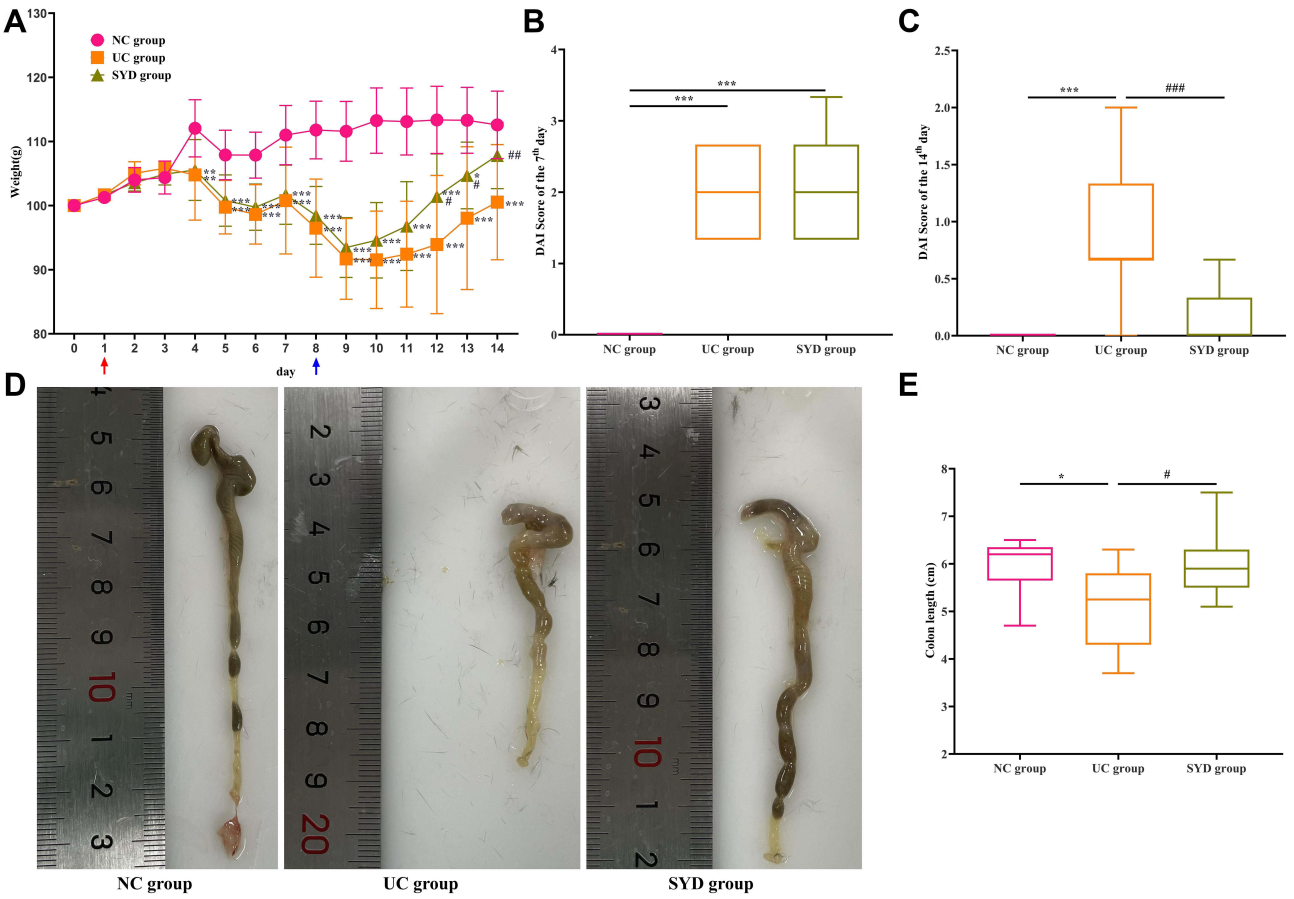

Figure 1 The weight, disease activity index (DAI) score, and colon length of mice in each group. (**A**) The changes in weight of mice throughout the experiment; (**B**) The DAI score of the 7th day in each group; (**C**) The DAI score of the 14th day in each group; (**D**) Typical colon anatomy of mice in each group; (**E**) The colon length of mice in each group. The red arrow means the first day of inducing UC by dextran sulfate sodium (DSS) and the blue arrow indicates the first day of medication. Compared with the NC group, ***P<0.001, **P<0.01, *P<0.05; compared with the UC group, ###P<0.001, ##P<0.01, #P<0.05.

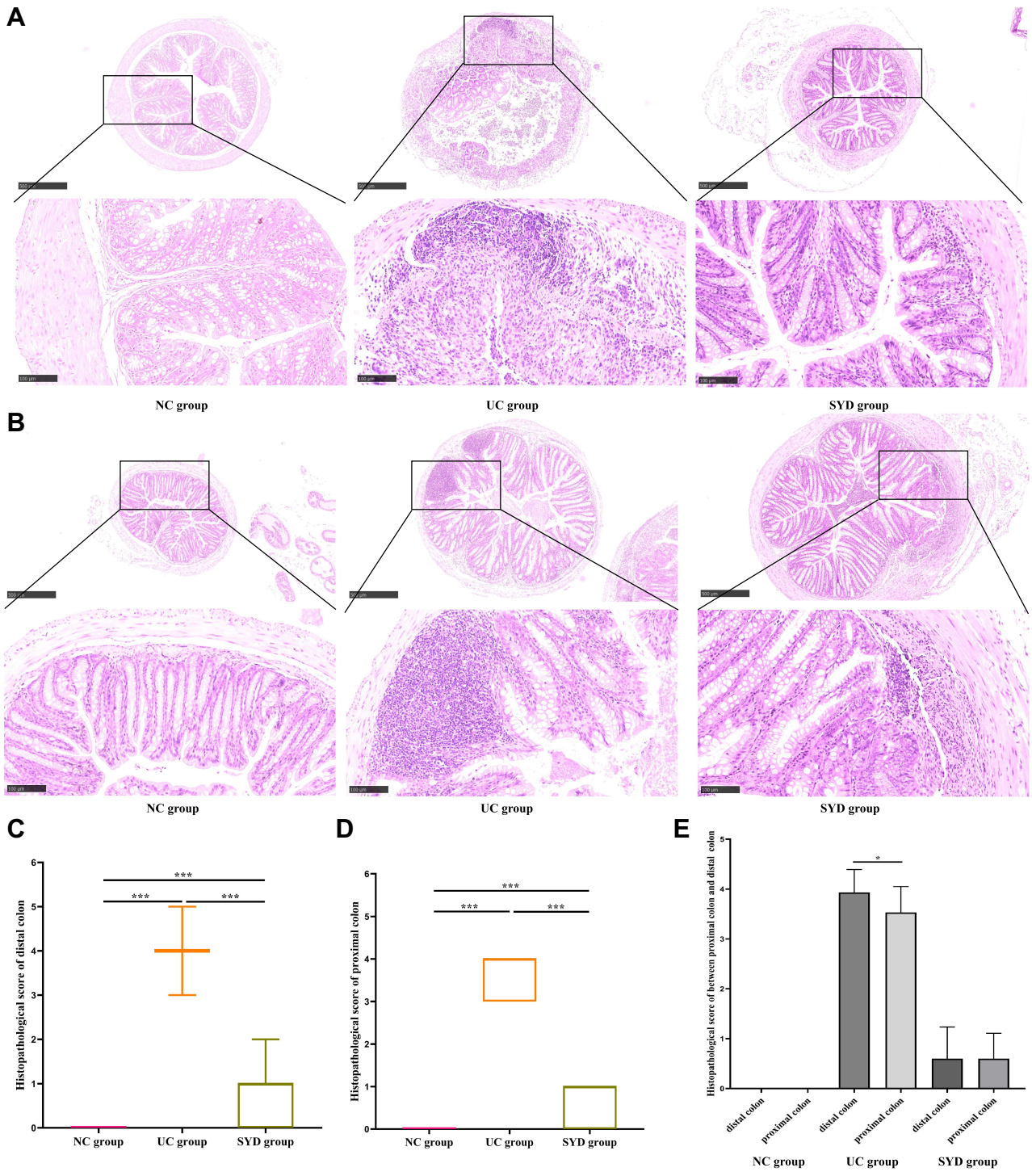

Figure 2 Histopathological changes and scores of colonic tissues of mice in each group. (**A**) Typical histopathological performance of distal colon (× 5 and × 20); (**B**) Typical histopathological performance of proximal colon (× 5 and × 20); (**C**) The histopathological score of distal colon; (**D**) The histopathological score of proximal colon; (**E**) The histopathological score between proximal colon and distal colon. *P<0.05; ***P<0.001.

mucosa. In addition, there was a loss of intact epithelium, and a large number of epithelial cells were destroyed. In the SYD group, destruction of the intestinal wall and inflammatory infiltration were milder than in the UC group.

The histopathological score of mice in the UC group was significantly higher than that of mice in the NC group (P<0.001). The histopathological score of mice in the SYD group was significantly lower than that of mice in the UC

group (P<0.001) (Figure 2C and D). In addition, in the UC group, the histopathological scores of distal colon were higher than proximal colon (P<0.05), while there was no difference in pathological scores between the proximal colon and distal colon in the NC group and SYD group (Figure 2E).

Analysis of Proximal Colon and Distal Colon Metabolite Profiles

UPLC-Q-TOF-MS was performed to identify the metabolic profiles of the proximal colon and distal colon samples collected from mice. As shown in Figure 3, the total ion current chromatograms (TICs) of the QC samples highly overlapped, indicating that the instrument was reliable and stable. Figure 4 indicates the representative TICs plots of each group, respectively.

PCA was used to distinguish the inherent trends within the colon metabolic data of each group. The score maps of PCA were shown in Figure 5, the tendency for segregation of the NC, UC, and SYD groups was observed, indicating significant variations in metabolites within the three groups. The loading maps of PCA were shown in Figure S4. Moreover, OPLS-DA was performed to force the classification of each component and facilitate the identification of differences and similarities between groups. The OPLS-DA models was validated by cross validation and CV-ANOVA. Validation parameters of OPLS-DA models (Q2 and R2) were arranged in Table 4, so were the p-values tested by CV-

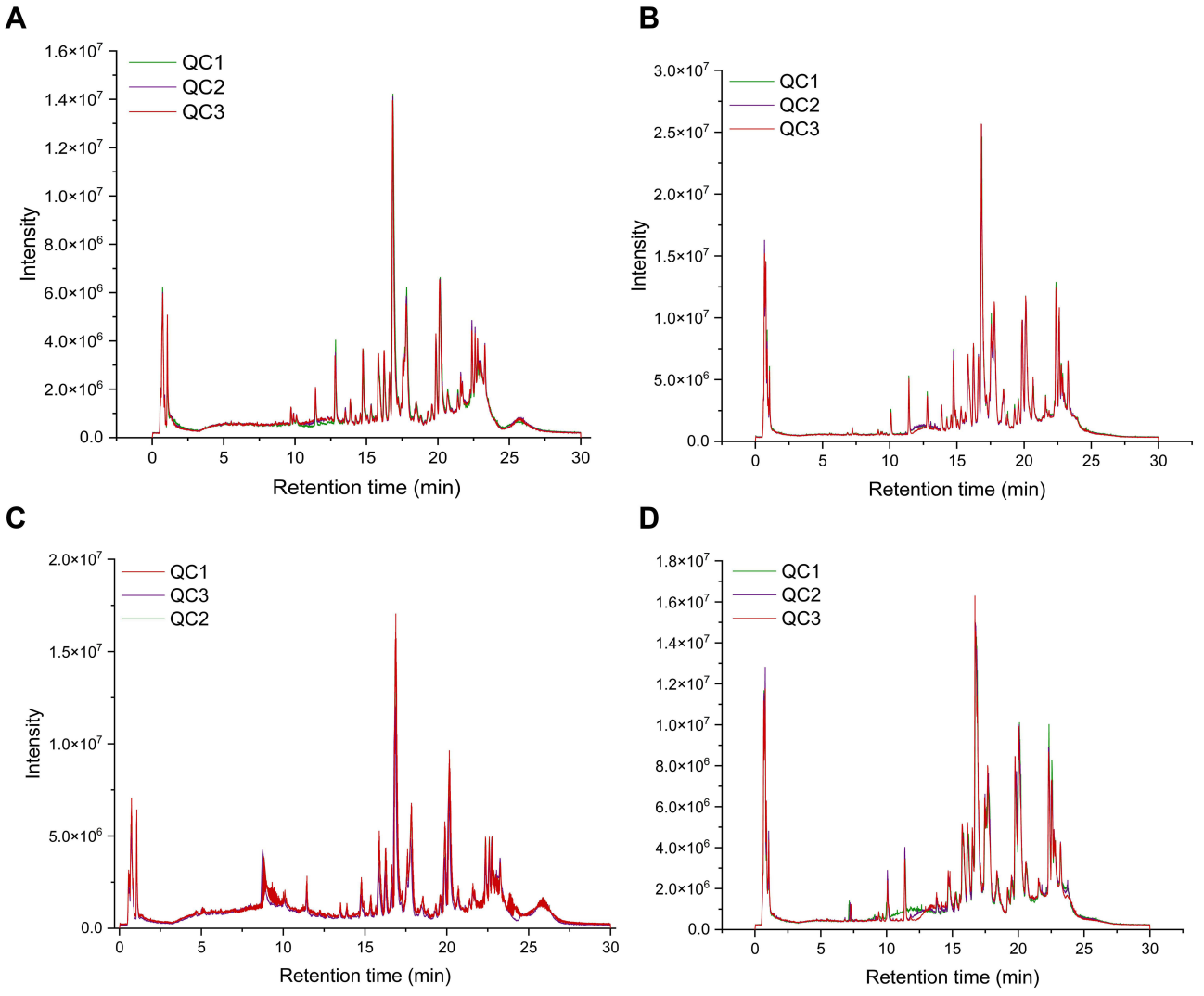

Figure 3 The total ion current chromatograms (TICs) of the quality control (QC) samples. (**A**) TICs of QC samples in the distal colon under positive ion mode; (**B**) TICs of QC samples in the distal colon under negative ion mode; (**C**) TICs of QC samples in the proximal colon under positive ion mode; (**D**) TICs of QC sample in the proximal colon under negative ion mode.

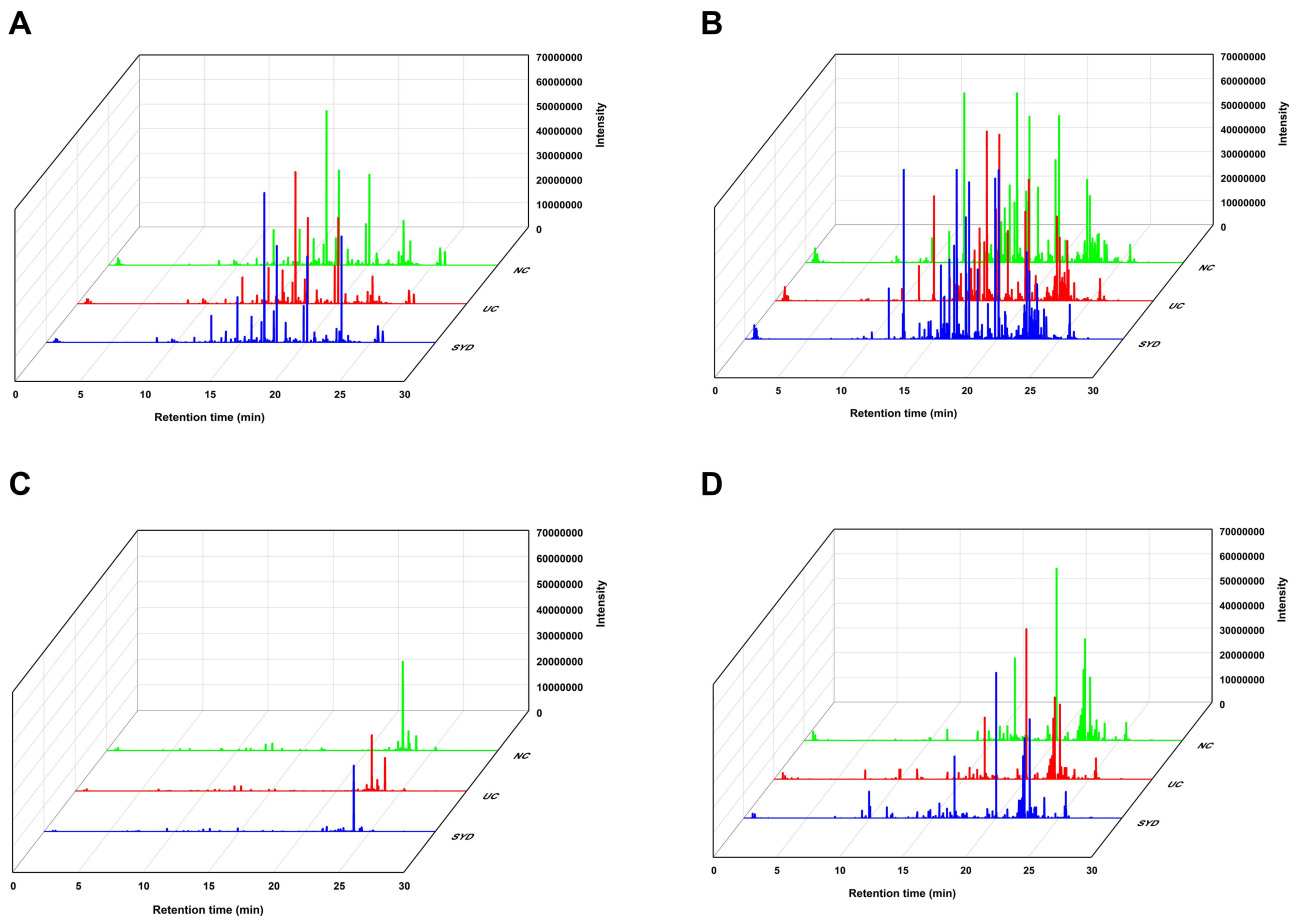

Figure 4 Indicates the representative total ion current chromatograms (TICs) plots of each group. (**A**) TICs of the distal colon under positive ion mode; (**B**) TICs of the distal colon under negative ion mode; (**C**) TICs of the proximal colon under positive ion mode; (**D**) TICs of the proximal colon under negative ion mode.

ANOVA. The p-values were <0.05 in all models, suggesting the models were valid. The OPLS-DA results showed that in the positive and negative ion modes, samples in each group were significantly clustered, and each group was significantly separated from another (Figure 6). The validation plots were shown in Figure 7.

Metabolites with VIP scores >1 in the OPLS-DA model and P<0.05 were considered significantly altered metabolic biomarkers. The volcano plots showed the differential metabolites between the comparison groups (Figure 8). In the distal colon samples, 102 significantly differential metabolites were identified between the NC and UC groups, and 54 significantly differential metabolites were identified between the UC and SYD groups (Tables S2 and S3). We further found that phosphatidic acid (PA) 20:0/12:0 and lysophosphatidylethanolamine (lysoPE) 0:0/22:5(4Z,7Z,10Z,13Z,16Z) significantly decreased after the induction of UC. After SYD intervention, the levels of these metabolites significantly increased. Moreover, three metabolites significantly increased in mice in the UC group compared with that in mice in the NC group; these metabolites were lactosylceramide (d18:1/12:0), erythrodiol 3-palmitate, and lysophosphatidylcholine (lysoPC) 22:2(13Z,16Z). After SYD treatment, these metabolites significantly decreased, as shown in Table 5 and Figure 9.

In the proximal colon samples, 112 significantly differential metabolites were identified between the NC and UC groups, and 75 significantly differential metabolites were identified between the UC and SYD groups (Tables S4 and S5). We further found that palmitic acid, cyclonormammein, monoacylglyceride (MG) 0:0/18:2(9Z,12Z)/0:0, 13S-hydroxyoctadecadienoic acid, and ceanothine C were significantly decreased after the induction of UC. After SYD intervention, the levels of these metabolites significantly increased. Moreover, tetracosahexaenoic acid, phosphatidylserine (PS) 18:0/22:6 (4Z,7Z,10Z,13Z,16Z,19Z), and diglyceride (DG) 14:0/20:2(11Z,14Z)/0:0 significantly increased in mice in the UC group

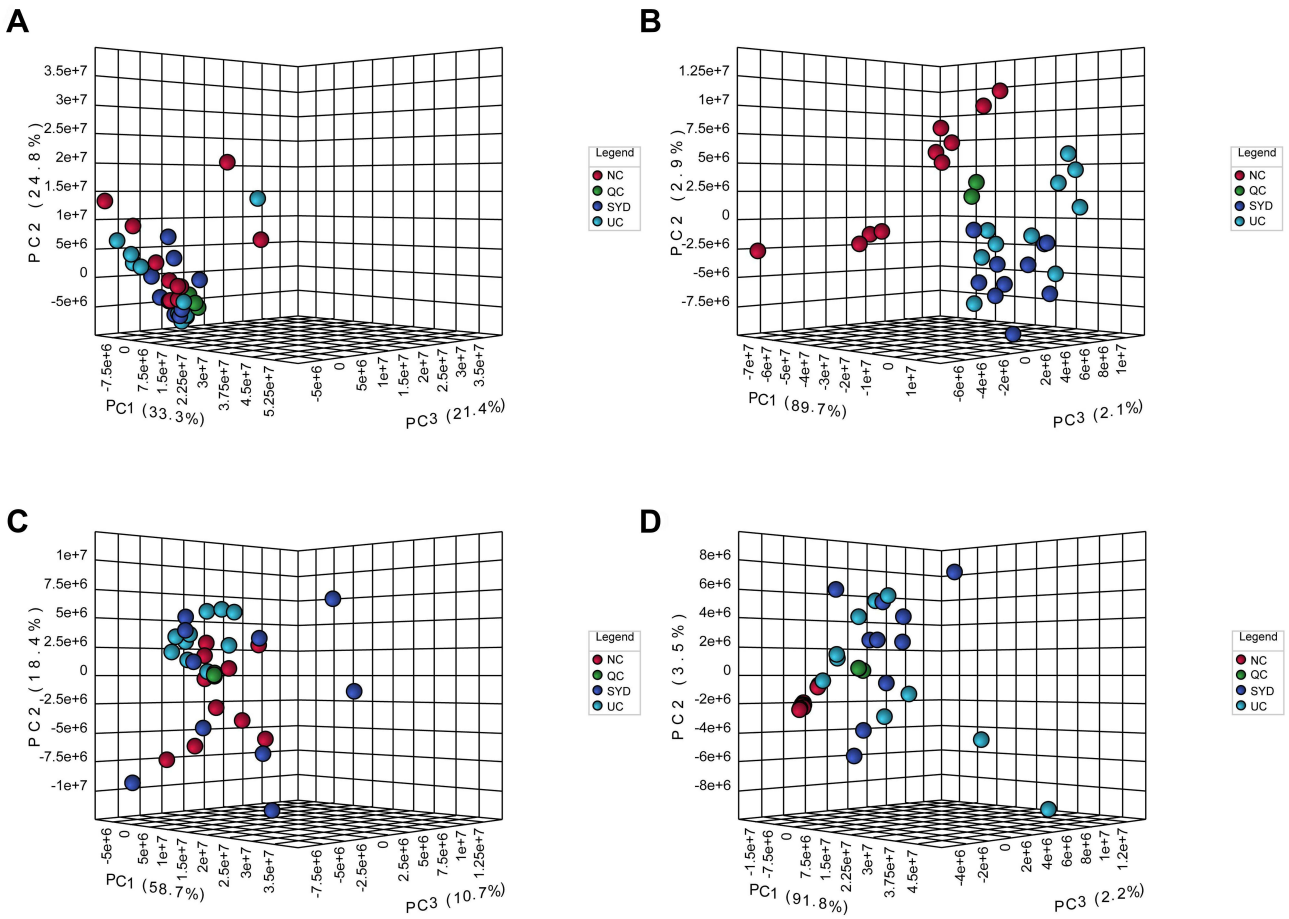

Figure 5 Multivariate statistical analysis of plasma metabolic profiles in mice of each group. (**A** and **B**) Three-dimensional plots of principal component analysis (PCA) of distal colon metabolic profile in mice of each group under negative and positive ion mode; (**C** and **D**) Three-dimensional plots of PCA of proximal colon metabolic profile in mice of each group under negative and positive ion mode.

when compared with that in mice in the NC group. After SYD treatment, these metabolites significantly decreased, as shown in Table 6 and Figure 10. Heatmaps of proximal colon and distal colon were used to visualize these significantly different metabolites (Figure 11A and B).

Table 4 Validation Parameters of OPLS-DA Models for Colon of Mice

Samples		NC vs UC		SYD vs UC	
		ESI(+)	ESI(-)	ESI(+)	ESI(-)
Distal colon	Significant components	3	6	4	3
	R2X	0.563	0.699	0.488	0.414
	Q2	0.893	0.85	0.711	0.581
	p	<0.05	<0.05	<0.05	<0.05
Proximal colon	Significant components	2	4	3	4
	R2X	0.815	0.571	0.63	0.517
	Q2	0.944	0.954	0.796	0.637
	p	<0.05	<0.05	<0.05	<0.05

Notes: ESI represents Electrospray Ionization; R2X represents the goodness of fit of models; Q2 represents the predictability of models; p values were calculated by CV-ANOVA; OPLS-DA model is valid when $p < 0.05$. NC vs UC: compare normal control group with UC model group; SYD vs UC: compare SYD treatment group with UC model group.

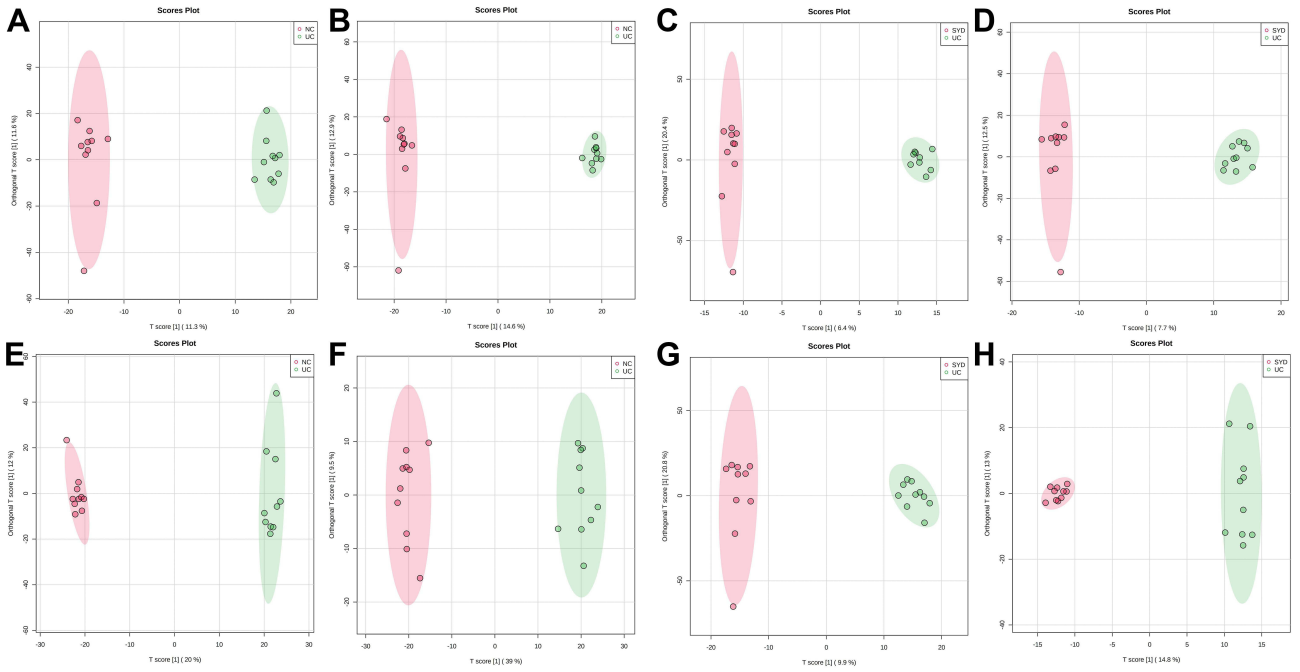

Figure 6 The orthogonal partial least squares discriminant analysis (OPLS-DA) diagrams between groups. (**A** and **B**) The OPLS-DA diagrams of distal colon between NC and UC group under negative and positive ion mode; (**C** and **D**) The OPLS-DA diagrams of distal colon between UC and SYD group under negative and positive ion mode; (**E** and **F**) The OPLS-DA diagrams of proximal colon between NC and UC group under negative and positive ion mode; (**G** and **H**) The OPLS-DA diagrams of proximal colon between UC and SYD group under negative and positive ion mode.

To further determine the metabolic pathways regulated by SYD, we performed the KEGG pathway enrichment analysis. In the distal colon samples, four pathways differed in the SYD and UC groups. The metabolic pathways included glycosphingolipid biosynthesis (globo and isoglobo series), sphingolipid metabolism (glycosphingolipid biosynthesis-ganglio series), and glycosphingolipid biosynthesis (lacto and neolacto series) (Figure 12A). These results indicate that SYD may regulate these pathways in the treatment of UC, and among them, the glycosphingolipid biosynthesis (lacto and neolacto series) pathway was the main metabolic pathway regulated by SYD. In the proximal colon samples, four pathways differed in the SYD and UC groups. The metabolic pathways include the biosynthesis of unsaturated fatty acids, fatty acid elongation, fatty acid degradation, and fatty acid biosynthesis (Figure 12B). These results indicate that SYD may regulate these pathways in the treatment of UC, and among them, the biosynthesis of unsaturated fatty acids pathway was the main metabolic pathway regulated by SYD.

Discussion

SYD is a traditional Chinese medicine prescription for treating many diseases, including UC and colorectal cancer.[29,30,65,66] In this study, we constructed a murine model of UC induced by DSS and proved that SYD was effective in UC mice, as it ameliorated the symptoms of UC, increased weight, improved colonic shortening, and reduced colonic damage. UPLC-Q-TOF-MS-based untargeted metabolomics was used to analyze the metabolite profiles of the proximal and distal colon and monitor and capture potential metabolic responses and biomarkers. Biomarkers have been used to label changes in systems, organs, tissues, cells, and subcellular structures or functions.[67] Although there are reports of potential blood biomarkers for UC, few studies have focused on UC biomarkers in tissue extracts, especially from the colon. Studies have demonstrated that most SCFAs are absorbed by the intestinal mucosa and have the highest concentration in colon tissue.[46–49] Therefore, studies on changes in intestinal metabolites in UC should focus on the colon tissue. Through metabolomic analysis of colon tissues, we identified five and eight metabolites that were up- or down-regulated by SYD in the distal colon and proximal colon, respectively.

In the distal colon, the levels of PA (20:0/12:0) and lysoPE (0:0/22:5(4Z,7Z,10Z,13Z,16Z)) decreased, and that of lactosylceramide (d18:1/12:0), erythrodiol 3-palmitate, and lysoPC (22:2(13Z,16Z)) increased in UC mice. However, the

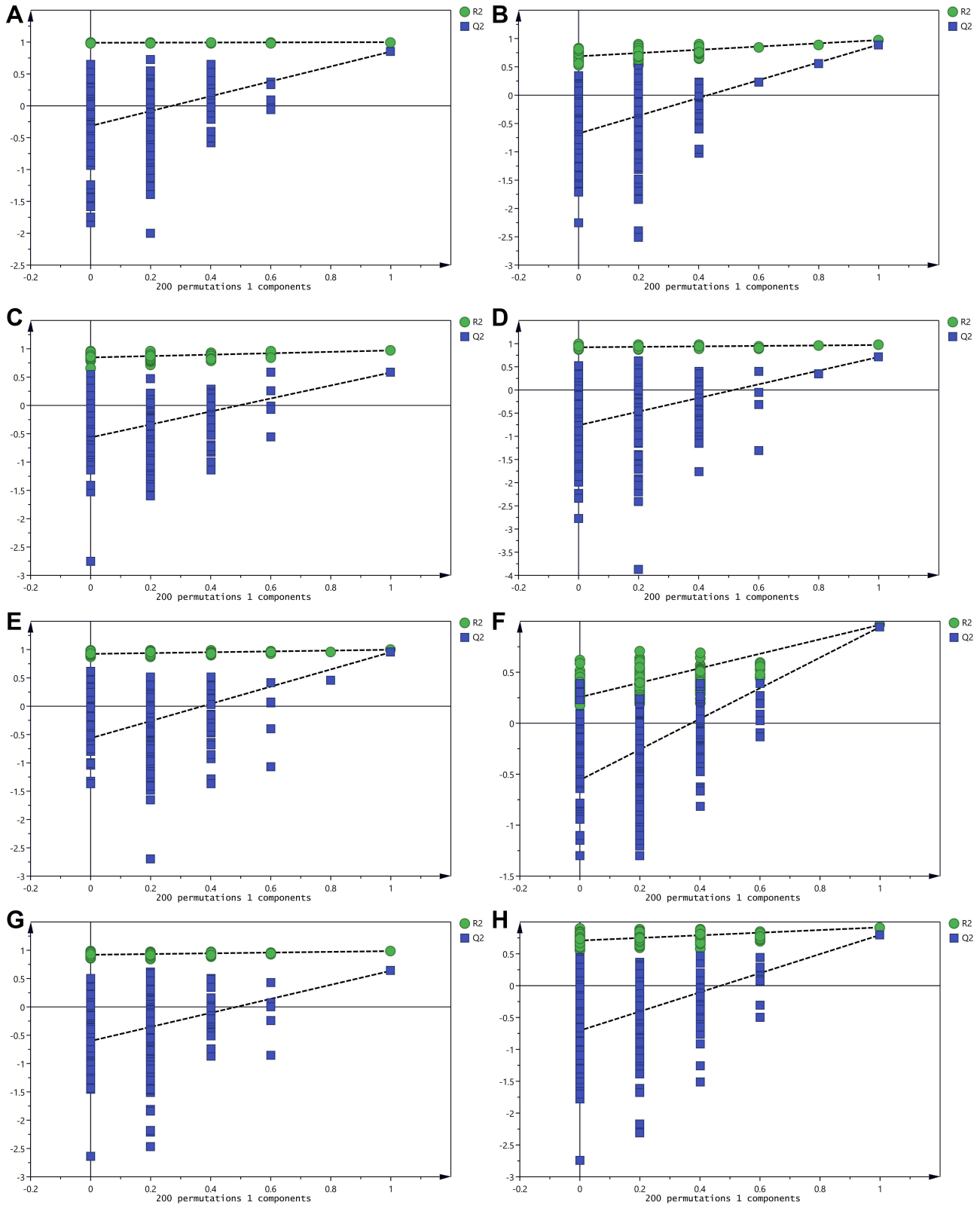

Figure 7 The validation of the orthogonal partial least squares discriminant analysis (OPLS-DA) model between groups. (**A** and **B**) The validation of the OPLS-DA model of distal colon between NC and UC group under negative and positive ion mode; (**C** and **D**) The validation of the OPLS-DA model of distal colon between UC and SYD group under negative and positive ion mode; (**E** and **F**) The validation of the OPLS-DA model of proximal colon between NC and UC group under negative and positive ion mode; (**G** and **H**) The validation of the OPLS-DA model of proximal colon between UC and SYD group under negative and positive ion mode.

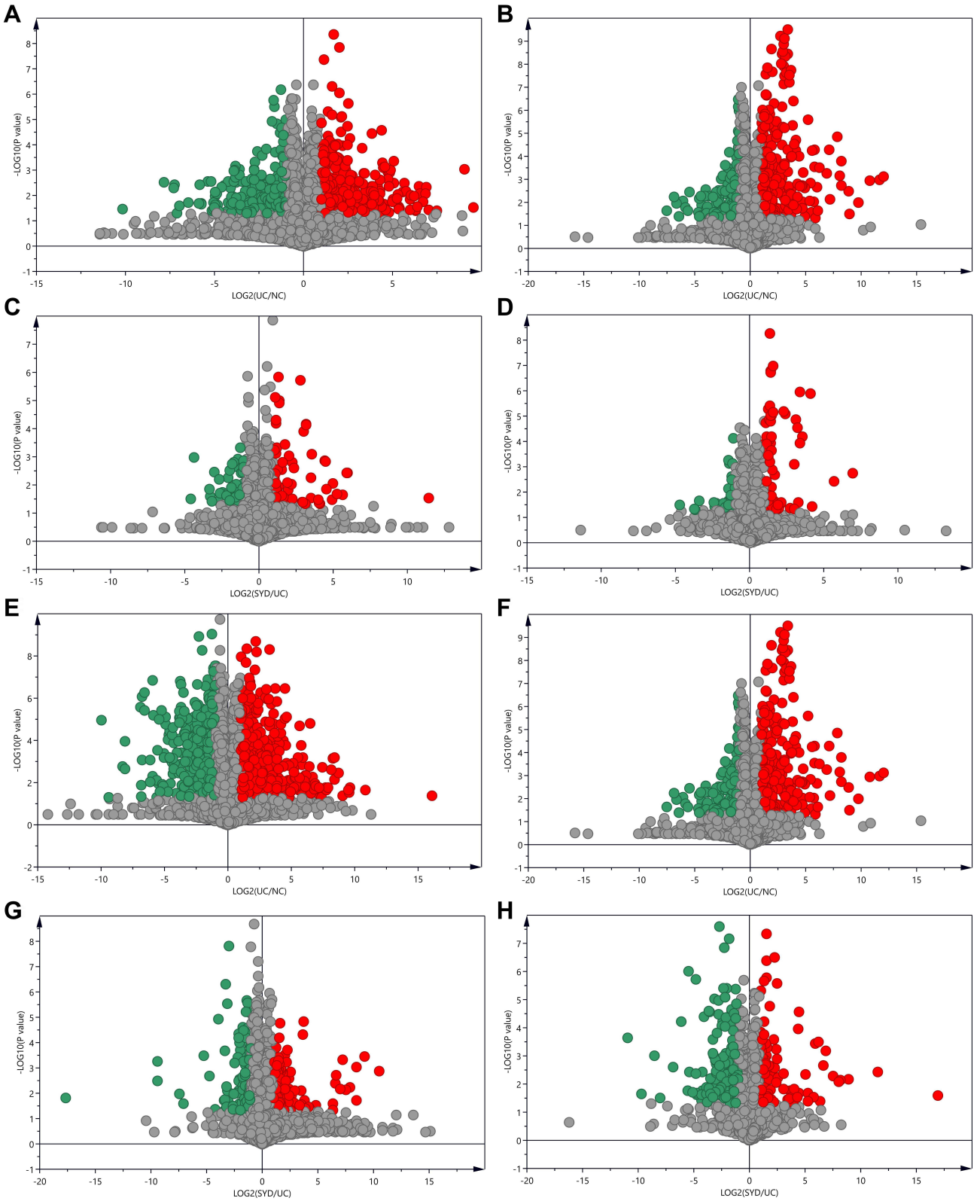

Figure 8 The volcano plots between groups. (**A** and **B**) The volcano plots of distal colon between NC and UC group under negative and positive ion mode; (**C** and **D**) The volcano plots of distal colon between UC and SYD group under negative and positive ion mode; (**E** and **F**) The volcano plots of proximal colon between NC and UC group under negative and positive ion mode; (**G** and **H**) The volcano plots of proximal colon between UC and SYD group under negative and positive ion mode.

Table 5 Metabolites of Distal Colon Regulated by SYD

Metabolites	UC vs NC			SYD vs UC		
	Ratio	P value	VIP Score	Ratio	P value	VIP Score
PA(20:0/12:0)	0.894941	0.0205379	1.32695	1.17827	0.00117747	2.91471
LysoPE(0:0/22:5(4Z,7Z,10Z,13Z,16Z))	0.568939	0.000222872	3.06501	1.2298	0.0471027	1.98451
Lactosylceramide (d18:1/12:0)	1.80105	0.00000986551	4.31211	0.737635	0.00094652	6.61917
Erythrodiol 3-palmitate	1.64825	0.00871662	2.08317	0.680032	0.0167853	2.70285
LysoPC(22:2(13Z,16Z))	1.36907	0.000079892	3.06522	0.848582	0.00772517	3.20606

content of these metabolites tended toward normal levels after SYD treatment. LysoPE is a lysoglycerophospholipid derived from phosphatidylethanolamines. The role of lysoPE in IBD was suggested when the rectal application of lysoPE reduced inflammation and mucosal damage in 2,4,6-trinitrobenzene sulfonic acid (TNBS)-induced colitis in rats.[68] Recently, Zou et al found that the levels of lysoPE 16:0 and lysoPE 18:1 decreased in fecal samples from patients with UC compared with those from controls, which is consistent with our results. In addition, they demonstrated that oral supplementation with lysoPE 18:1 could regulate the expression of occludin, claudin-1, and ZO-1, and ameliorate intestinal permeability.[69] In our study, we found that lysoPE levels in the distal colon tissue decreased after UC modeling, whereas SYD increased lysoPE levels, indicating that SYD can regulate the intestinal mucosal barrier by regulating the level of lysoPE, thereby improving intestinal mucosal damage. Phosphatidylcholine (PC) is a phospholipid that accounts for more than 70% of total phospholipids in the intestinal mucus layer, and it has been shown to possess anti-inflammatory effects.[70,71] In contrast, lysoPC derived from PC has been reported to be pro-inflammatory.[72,73] LysoPC exacerbates inflammatory response by promoting the expression of growth factors, chemotaxis factors, and endothelial

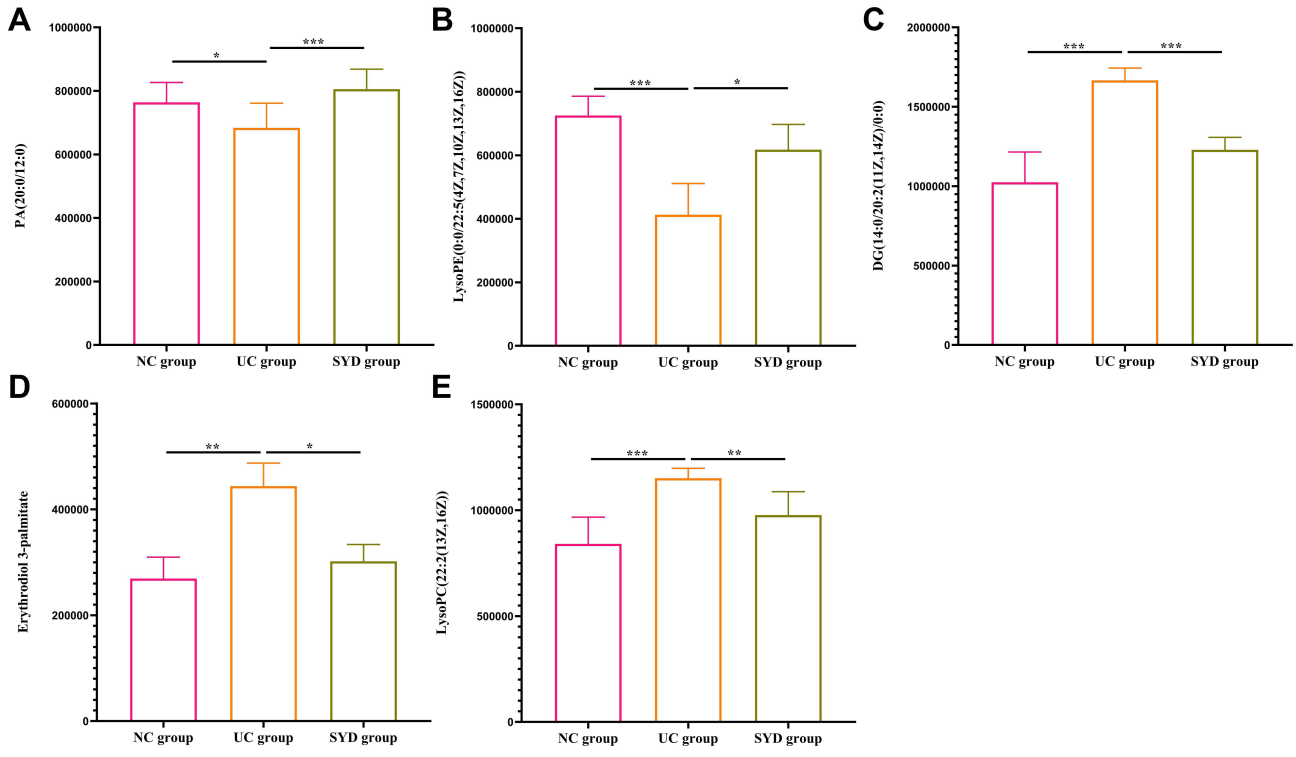

Figure 9 The abundance of differential metabolites in distal colon. (**A**) The abundance of PA(20:0/12:0) in each group; (**B**) The abundance of LysoPE(0:0/22:5 (4Z,7Z,10Z,13Z,16Z)) in each group; (**C**) The abundance of Lactosylceramide (d18:1/12:0) in each group; (**D**) The abundance of Erythrodiol 3-palmitate in each group; (**E**) The abundance of LysoPC(22:2(13Z,16Z)) in each group. *P<0.05, **P<0.01, ***P<0.001.

Table 6 Metabolites of Proximal Colon Regulated by SYD

Metabolites	UC vs NC			SYD vs UC		
	Ratio	P value	VIP Score	Ratio	P value	VIP Score
Palmitic acid	0.730117	0.0000355773	2.5296	1.39055	0.000674936	3.1886
Cyclonormammein	0.791462	0.00004865	1.1149	1.35935	0.000759234	1.58454
MG(0:0/18:2(9Z,12Z)/0:0)	0.487968	0.000000223837	1.87145	1.41523	0.0118603	1.71807
13S-hydroxyoctadecadienoic acid	0.565985	0.000320875	1.78446	1.52314	0.00667784	1.9476
Ceanothine C	0.333676	0.0313459	1.54408	3.15366	0.0142017	2.26543
Tetracosahexaenoic acid	1.28607	0.00060681	2.31135	0.85079	0.0132296	2.31811
PS(18:0/22:6(4Z,7Z,10Z,13Z,16Z,19Z))	1.13411	0.0314816	1.92516	0.815578	0.011245	3.18233
DG(14:0/20:2(11Z,14Z)/0:0)	2.00355	0.0000000862851	1.53319	0.8513	0.0339027	1.21406

cell adhesion molecules.[72] It increases intestinal permeability and bacterial translocation.[74] Patients with UC were found to have decreased PC levels and increased lysoPC levels, and PC supplementation alleviated inflammation.[75,76] In TNBS-induced colitis mice and DSS-induced colitis mice, lysoPC was elevated in serum samples. PC and lysoPC levels are strongly associated with UC, and the lysoPC/PC ratio is particularly important in improving intestinal permeability.[77,78] Our results confirmed that SYD could regulate lysoPC levels and exert an anti-inflammatory effect in the distal colon. Lactosylceramide (LacCer) is a glycosphingolipid.[79] Glycosphingolipids are a class of membrane molecules that regulate membrane fluidity, receptor protein function, and cell adhesion.[80] LacCer plays an important role in the human body by taking part in the conduction of various signals.[81,82] It was found to be elevated primarily in Crohn's disease (CD) in a study of serum metabolomics in children with IBD, and it was suggested that serum LacCer may be a potential biomarker that could differentiate children with IBD from healthy individuals and distinguish the subtypes of IBD.[83] Another study also demonstrated that serum LacCer 18:1/16:0 could significantly discriminate CD from UC in children.[84] Both studies involved children; therefore, more studies are required to demonstrate the role of LacCer in adult IBD patients. Interestingly, in inflamed colon tissue of adult patients with UC, the level of LacCer was increased,[85] which was consistent with our results. Therefore, the role of LacCer in UC warrants further study.

In the proximal colon, the level of palmitic acid, cyclonormammein, MG (0:0/18:2(9Z,12Z)/0:0), 13S-hydroxyoctadecadienoic acid, and ceanothine C decreased, whereas that of tetracosahexaenoic acid, PS (18:0/22:6 (4Z,7Z,10Z,13Z,16Z,19Z)), and DG (14:0/20:2(11Z,14Z)/0:0) increased in UC mice. The levels of these metabolites tended to normalize after SYD treatment. The 13S-hydroxyoctadecadienoic acid (13S-HODE) is a derivative of linoleic acid and the predominant regulator of inflammation in different cell systems, such as endothelial cells.[86–88] However, the role of 13S-HODE in UC has not been studied thoroughly. Interestingly, a recent study found that black raspberries increased the levels of 13S-HODE in interleukin (IL)-10 KO mice and played a role in the treatment of UC.[89] This is consistent with our findings; SYD increased the level of 13S-HODE in the proximal colon, indicating that it plays a role in the treatment of UC mainly by regulating13S-HODE levels in the proximal colon. PS is participates in inflammation and can initiate platelet activation and apoptosis. It is considered an upstream immune checkpoint that suppresses the development of immunity.[90] Researchers also found that an increased level of PS was related to the activation of platelets, which could increase thrombotic risk in patients with IBD.[91] In addition, Iwatani et al reported a significant increase in PS with respect to IBD activity,[92] which is consistent with our findings. We found that in UC mice, the levels of PS increased, and SYD decreased PS levels, demonstrating that SYD may reduce thrombotic risk in UC. Regarding palmitic acid and DG (14:0/20:2(11Z,14Z)/0:0), palmitic acid is a long-chain saturated fatty acid found in animals, plants, and microorganisms. At the intestinal level, palmitic acid induces monocyte activation and stimulates pro-inflammatory responses.[93,94] Ghezzal et al found that the intake of palm oil provokes an increase in intestinal permeability and loss of several tight junction proteins. They also found that palmitic acid increased the expression and secretion of pro-inflammatory cytokines and exerted its harmful effects on epithelial cells.[95] DG (14:0/20:2(11Z,14Z)/0:0) is a diglyceride and diacylglycerol, which can inhibit the secretion of bile acids and is used to prevent and treat diarrhea.[96] Murase et al have reported that diacylglycerol can inhibit the occurrence of colitis.[97] Our study found that the palmitic acid level in the proximal colon decreased and that

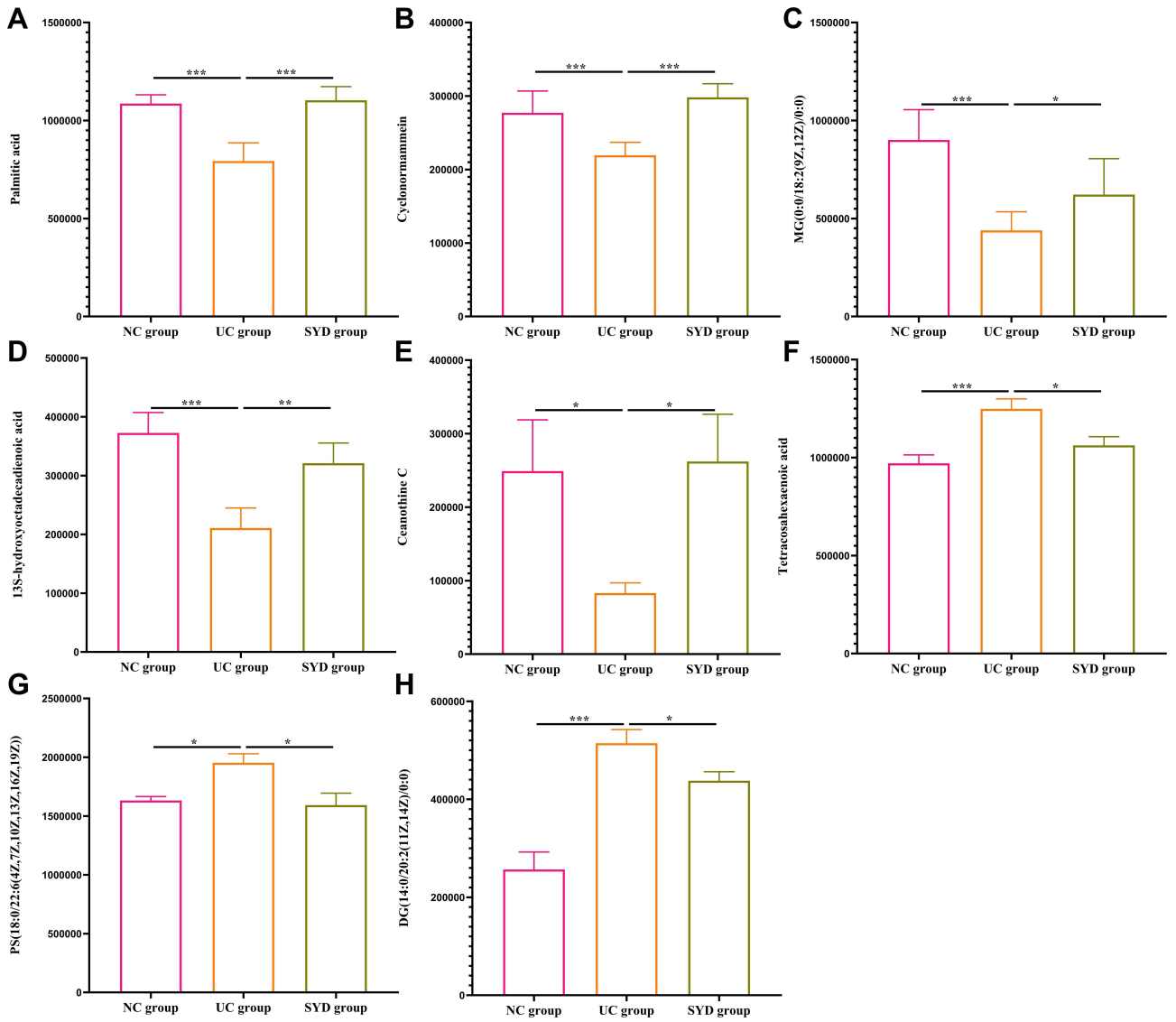

Figure 10 The abundance of differential metabolites in proximal colon. (**A**) The abundance of Palmitic acid in each group; (**B**) The abundance of Cyclonormammein in each group; (**C**) The abundance of MG(0:0/18:2(9Z,12Z)/0:0) in each group; (**D**) The abundance of 13S-hydroxyoctadecadienoic acid in each group; (**E**) The abundance of Ceanothine C in each group; (**F**) The abundance of Tetracosahexaenoic acid in each group; (**G**) The abundance of PS(18:0/22:6(4Z,7Z,10Z,13Z,16Z,19Z)) in each group; (**H**) The abundance of DG(14:0/20:2(11Z,14Z)/0:0) in each group. *P<0.05, **P<0.01, ***P<0.001.

of DG (14:0/20:2 (11Z, 14 Z)/0:0) increased after UC modeling. This indicates that the inflammation in the proximal colon was not severe; however, metabolic disorders still existed. SYD can regulate the levels of palmitic acid and DG (14:0/20:2 (11Z,14Z)/0:0) to normal levels, indicating a specific role of SYD in regulating the disturbance of intestinal metabolites.

Relevant reports on the role of PA (20:0/12:0), erythrodiol 3-palmitate, cyclonormammein, MG (0:0/18:2(9Z,12Z)/0:0), and ceanothine C in UC are few; therefore, the role of these metabolites requires further study. Further analysis of the metabolic pathways regulated by SYD revealed that, in the distal colon, SYD regulated the glycosphingolipid biosynthesis (lacto and neolacto series) pathway. In the proximal colon, the pathway for the biosynthesis of unsaturated fatty acids was the main metabolic pathway regulated by SYD. From the differential metabolites and metabolic pathways, we found that the metabolite environments in the proximal colon and distal colon of the DSS-induced colitis model mice were different, and there were different metabolic disorders present. We observed that in the DSS-induced colitis mouse model, the levels of inflammatory metabolites in the distal colon were higher than that in the proximal colon, indicating that inflammation in the distal colon was more serious than that in the proximal colon. The effect of SYD in the treatment of UC is mediated by

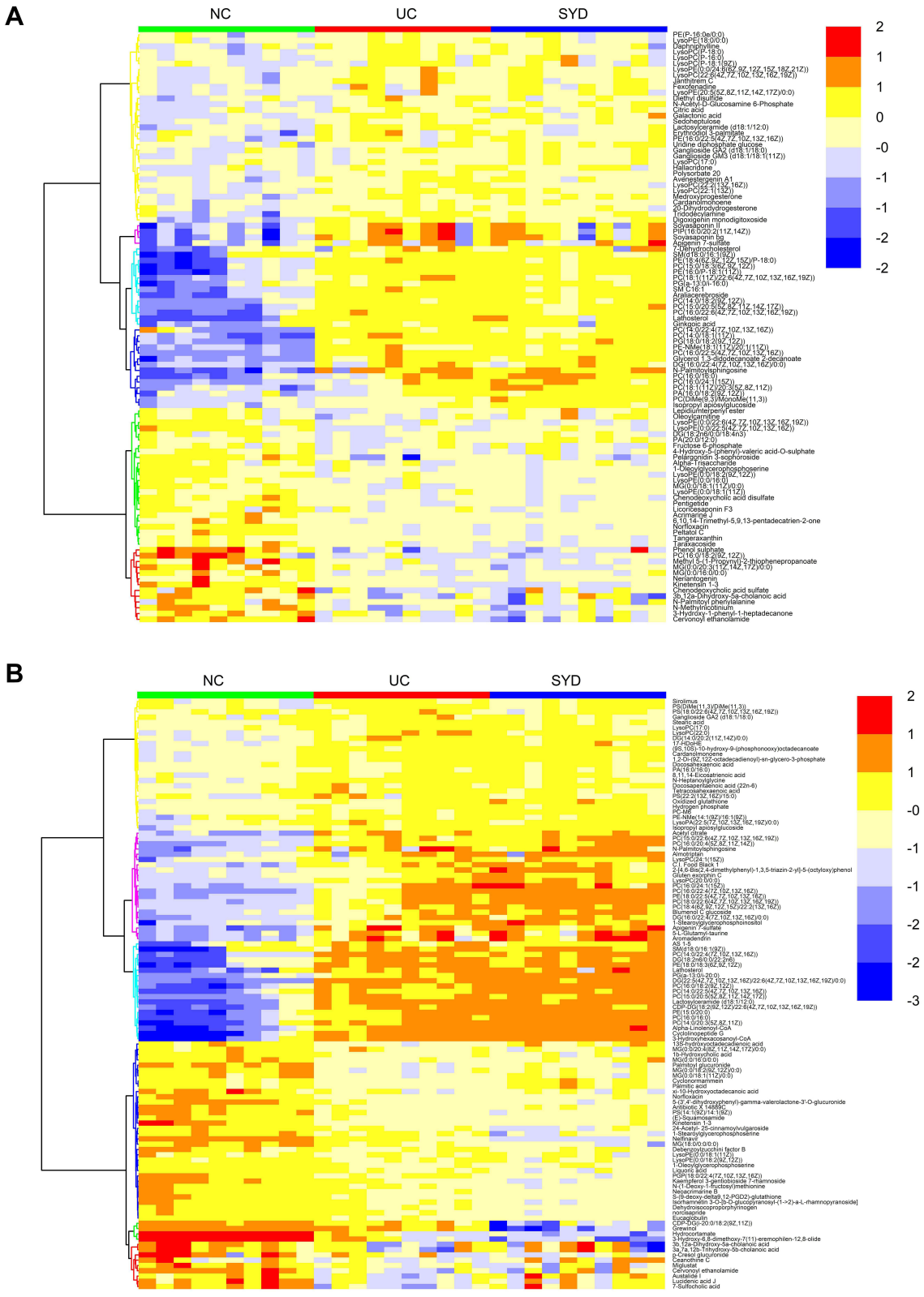

Figure 11 The heat map among groups. (**A**) The heat map of distal colon among groups; (**B**) The heat map of proximal colon among groups.

the regulation of metabolites in the distal colon. Our findings are also helpful in understanding the pathogenesis of UC, as UC is characterized by chronic mucosal inflammation beginning in the rectum and extending proximally to a variable distance. Moreover, previous studies have found that the assessment of the severity of inflammation in the left-sided colon

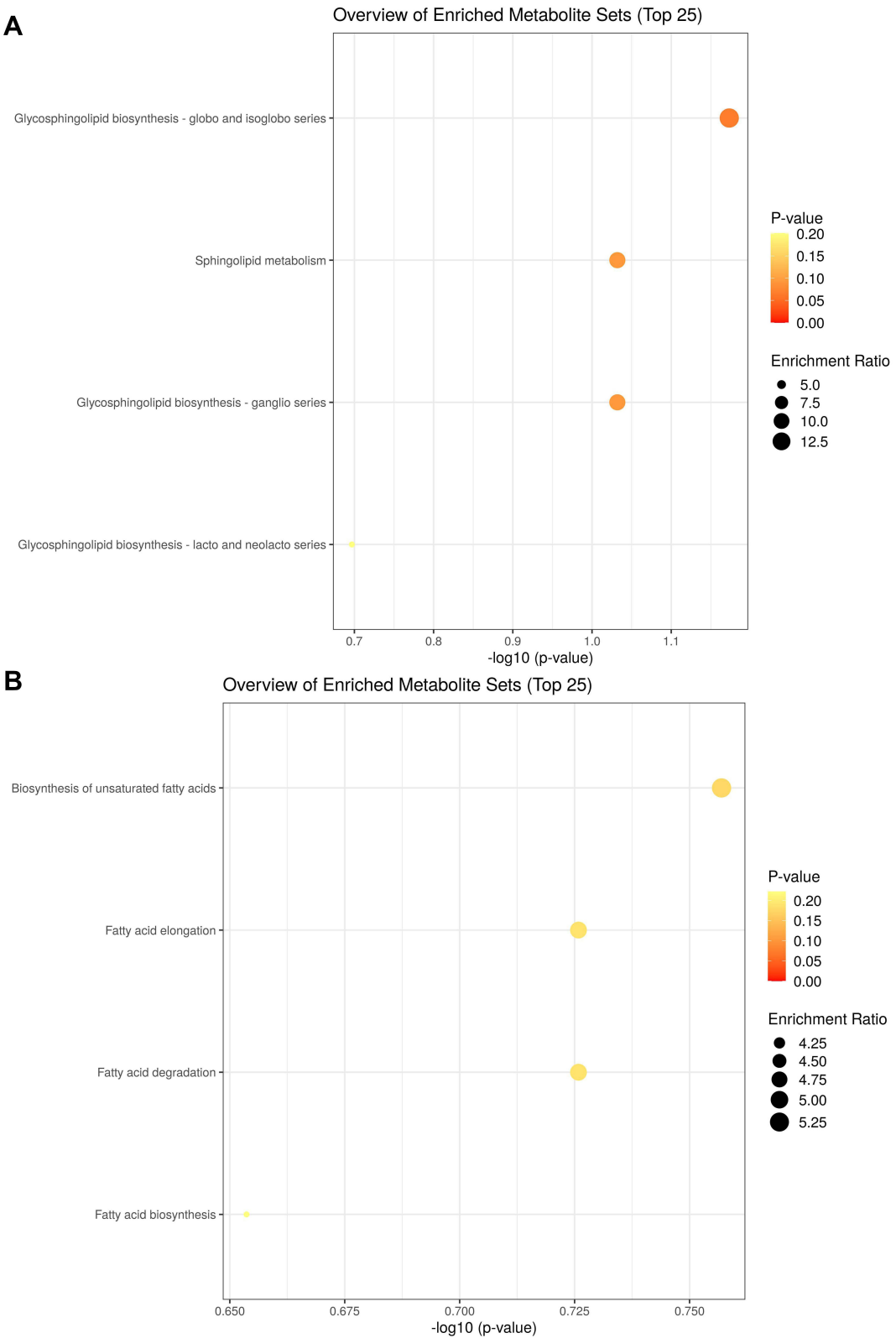

Figure 12 The metabolic pathways regulated by SYD. (**A**) The metabolic pathways of the distal colon regulated by SYD; (**B**) The metabolic pathways of the proximal colon regulated by SYD.

had excellent accuracy for the detection of right-sided histologic disease activity.[98] Our findings are helpful for more accurate follow-up studies on UC and suggest that the effects of drugs on the proximal colon and distal colon should be studied separately to provide more precise evidence.

Conclusion

Our study found that different metabolic disorders exist in the proximal colon and distal colon and demonstrated that SYD intervention could ameliorate DSS-induced colonic damage, which may be attributed to SYD targeting specific metabolites and pathways. Our findings may help clarify the detailed mechanism of SYD in the treatment of UC and provide an important reference for further studies.

Abbreviations

UC, ulcerative colitis; IBD, inflammatory bowel disease; SYD, Shaoyao Decoction; DSS, dextran sulfate sodium; SCFAs, short chain fatty acids; IL, interleukin; DAI, disease activity index; UPLC-Q-TOF-MS, ultra performance liquid chromatography combined with quadrupole-time-of-flight mass spectrometry; GC-MS, gas chromatography-mass spectrometry; NMR, nuclear magnetic resonance; NC group, normal control group; UC group, UC model group; SYD group, SYD treatment group; H&E, Hematoxylin and Eosin; QC, Quality Control; PCA, principal component analysis; OPLS-DA, orthogonal partial least squares discriminant analysis; KEGG, Kyoto Encyclopedia of Genes and Genomes; VIP, variable importance in the projection; TICs, total ion chromatograms; PA, phosphatidic acid; lysoPE, lysophosphatidylethanolamine; lysoPC, lysophosphatidylcholine; MG, monoacylglyceride; PS, phosphatidylserine; DG, diglyceride; PC, phosphatidylcholine; TNBS, 2,4,6-trinitrobenzene sulfonic acid; LacCer, Lactosylceramide; CD, Crohn's disease; 13S-HODE, 13S-hydroxyoctadecadienoic acids.

Data Sharing Statement

The data used to support the findings of this study are included within the article. The datasets used and/or analyzed during the current study are available from the corresponding author upon reasonable request.

Ethical Approval

The experimental procedures were approved by the Experimental Animal Ethics Committee of Zhejiang Chinese Medical University (IACUC-20210531-02). Ethics Committee of The Second Affiliated Hospital of Zhejiang Chinese Medical University has reviewed our current study, the human data only involves publicly available data, so, the ethics committee agreed to exempt the our study from the application for ethics review.

Funding

This research was supported by Zhejiang Province Traditional Chinese Medicine Science and Technology Project (No: 2021ZQ042), Zhejiang Traditional Chinese Medicine Administration (No: 2020ZZ010), and Zhejiang Province Natural Science Foundation (No: LY21H270007).

Disclosure

The authors report no conflicts of interest in this work.

References

1. Kobayashi T, Siegmund B, Le Berre C, et al. Ulcerative colitis. *Nat Rev Dis Primers*. 2020;6(1):74. doi:10.1038/s41572-020-0205-x
2. Sreedhar R, Arumugam S, Thandavarayan RA, Karuppagounder V, Watanabe K. Curcumin as a therapeutic agent in the chemoprevention of inflammatory bowel disease. *Drug Discov Today*. 2016;21(5):843–849. doi:10.1016/j.drudis.2016.03.007
3. Ivanov II, Atarashi K, Manel N, et al. Induction of intestinal Th17 cells by segmented filamentous bacteria. *Cell*. 2009;139(3):485–498. doi:10.1016/j.cell.2009.09.033
4. Neurath MF. New targets for mucosal healing and therapy in inflammatory bowel diseases. *Mucosal Immunol*. 2014;7(1):6–19. doi:10.1038/mi.2013.73
5. Du L, Ha C. Epidemiology and pathogenesis of ulcerative colitis. *Gastroenterol Clin North Am*. 2020;49(4):643–654. doi:10.1016/j.gtc.2020.07.005
6. He J, Song Y, Li G, et al. Fbxw7 increases CCL2/7 in CX3CR1hi macrophages to promote intestinal inflammation. *J Clin Invest*. 2019;129(9):3877–3893. doi:10.1172/JCI123374

7. Kaplan GG, Windsor JW. The four epidemiological stages in the global evolution of inflammatory bowel disease. *Nat Rev Gastroenterol Hepatol*. 2021;18(1):56–66. doi:10.1038/s41575-020-00360-x
8. Ng SC, Shi HY, Hamidi N, et al. Worldwide incidence and prevalence of inflammatory bowel disease in the 21st century: a systematic review of population-based studies. *Lancet*. 2017;390(10114):2769–2778. doi:10.1016/S0140-6736(17)32448-0
9. Ananthakrishnan AN, Kaplan GG, Ng SC. Changing global epidemiology of inflammatory bowel diseases: sustaining health care delivery into the 21st century. *Clin Gastroenterol Hepatol*. 2020;18(6):1252–1260. doi:10.1016/j.cgh.2020.01.028
10. Ng SC, Kaplan GG, Tang W, et al. Population density and risk of inflammatory bowel disease: a prospective population-based study in 13 countries or regions in Asia-Pacific. *Am J Gastroenterol*. 2019;114(1):107–115. doi:10.1038/s41395-018-0233-2
11. Parente JM, Coy CS, Campelo V, et al. Inflammatory bowel disease in an underdeveloped region of Northeastern Brazil. *World J Gastroenterol*. 2015;21(4):1197–1206. doi:10.3748/wjg.v21.i4.1197
12. Panés J, Alfaro I. New treatment strategies for ulcerative colitis. *Expert Rev Clin Immunol*. 2017;13(10):963–973. doi:10.1080/1744666X.2017.1343668
13. Frias Gomes C, Chapman TP, Satsangi J. De-escalation of medical therapy in inflammatory bowel disease. *Curr Opin Pharmacol*. 2020;55:73–81. doi:10.1016/j.coph.2020.09.014
14. Quezada SM, McLean LP, Cross RK. Adverse events in IBD therapy: the 2018 update. *Expert Rev Gastroenterol Hepatol*. 2018;12(12):1183–1191. doi:10.1080/17474124.2018.1545574
15. Mourad AA, Boktor MN, Yilmaz-Demirdag Y, Bahna SL. Adverse reactions to infliximab and the outcome of desensitization. *Ann Allergy Asthma Immunol*. 2015;115(2):143–146. doi:10.1016/j.anai.2015.06.004
16. Moćko P, Kawalec P, Pilc A. Safety profile of biologic drugs in the treatment of inflammatory bowel diseases: a systematic review and network meta-analysis of randomized controlled trials. *Clin Drug Investig*. 2017;37(1):25–37. doi:10.1007/s40261-016-0459-y
17. Casas AI, Hassan AA, Larsen SJ, et al. From single drug targets to synergistic network pharmacology in ischemic stroke. *Proc Natl Acad Sci U S A*. 2019;116(14):7129–7136. doi:10.1073/pnas.1820799116
18. Hu J, Huang H, Che Y, et al. Qingchang Huashi Formula attenuates DSS-induced colitis in mice by restoring gut microbiota-metabolism homeostasis and goblet cell function. *J Ethnopharmacol*. 2021;266:113394. doi:10.1016/j.jep.2020.113394
19. Ye XX, Xia LT, Ren HM, et al. Research progress on processing history evolution, chemical constituents and pharmacological action of Paeoniae Radix Alba. *Chin Trad Herbal Drugs*. 2020;51(07):1951–1969.
20. Chao WW, Lin BF. Bioactivities of major constituents isolated from Angelica sinensis (Danggui). *Chin Med*. 2011;6:29. doi:10.1186/1749-8546-6-29
21. Yarla NS, Bishayee A, Sethi G, et al. Targeting arachidonic acid pathway by natural products for cancer prevention and therapy. *Semin Cancer Biol*. 2016;40–41:48–81. doi:10.1016/j.semcancer.2016.02.001
22. Hesari A, Ghasemi F, Cicero AFG, et al. Berberine: a potential adjunct for the treatment of gastrointestinal cancers? *J Cell Biochem*. 2018;119 (12):9655–9663. doi:10.1002/jcb.27392
23. Pirillo A, Catapano AL. Berberine, a plant alkaloid with lipid- and glucose-lowering properties: from in vitro evidence to clinical studies. *Atherosclerosis*. 2015;243(2):449–461. doi:10.1016/j.atherosclerosis.2015.09.032
24. Liao H, Ye J, Gao L, Liu Y. The main bioactive compounds of Scutellaria baicalensis Georgi. for alleviation of inflammatory cytokines: a comprehensive review. *Biomed Pharmacother*. 2021;133:110917. doi:10.1016/j.biopha.2020.110917
25. Zhu Y, Liu QX, Wanf SH, Liu DM, Chen L. Clinical observation on the treatment of 35 cases of large intestine damp-heat ulcerative colitis with Shaoyao Decoction combined with mesalazine. *World J Integr Tradit WestMed*. 2021;16(09):1653–1657.
26. Li XF, Wang YQ, Ye HX. Curative Observation of modified Shaoyao Tang for ulcerative colitis in active stage and its effect on pathological changes of colon. *J New Chin Med*. 2021;53(23):59–62.
27. Shi XL. Clinical observation of Shaoyao decoction combined with aidisha in the treatment of ulcerative colitis. *Nei Mongol JTrad Chin Med*. 2021;40(12):20–22.
28. Yu R, Yao GJ. Clinical effect of Jianpishaoyao decoction on ulcerative colitis of damp-heat accumulation type. *Chin j Clin Ration Drug Use*. 2021;14(36):21–24.
29. Chi H, Wang D, Chen M, et al. Shaoyao decoction inhibits inflammation and improves intestinal barrier function in mice with dextran sulfate sodium-induced colitis. *Front Pharmacol*. 2021;12:524287. doi:10.3389/fphar.2021.524287
30. Wei YY, Fan YM, Ga Y, Zhang YN, Han JC, Hao ZH. Shaoyao decoction attenuates DSS-induced ulcerative colitis, macrophage and NLRP3 inflammasome activation through the MKP1/NF-κB pathway. *Phytomedicine*. 2021;92:153743. doi:10.1016/j.phymed.2021.153743
31. Cao H, Wu DS, Zhang Y, Zou B, Chen YY, Li ZH. Effects of Shaoyao Decoction on intestinal flora of ulcerative colitis rats based on high-throughput sequencing technology. *Chin J Inf Tradit Chin Med*. 2021;28(1):61–66.
32. Rooks MG, Garrett WS. Gut microbiota, metabolites and host immunity. *Nat Rev Immunol*. 2016;16(6):341–352. doi:10.1038/nri.2016.42
33. Dorrestein PC, Mazmanian SK, Knight R. Finding the missing links among metabolites, microbes, and the host. *Immunity*. 2014;40(6):824–832. doi:10.1016/j.immuni.2014.05.015
34. Donia MS, Fischbach MA. Human microbiota. Small molecules from the human microbiota. *Science*. 2015;349(6246):1254766. doi:10.1126/science.1254766
35. Postler TS, Ghosh S. Understanding the Holobiont: how Microbial Metabolites Affect Human Health and Shape the Immune System. *Cell Metab*. 2017;26(1):110–130. doi:10.1016/j.cmet.2017.05.008
36. Nicholson JK, Holmes E, Kinross J, et al. Host-gut microbiota metabolic interactions. *Science*. 2012;336(6086):1262–1267. doi:10.1126/science.1223813
37. Sun M, Wu W, Liu Z, Cong Y. Microbiota metabolite short chain fatty acids, GPCR, and inflammatory bowel diseases. *J Gastroenterol*. 2017;52 (1):1–8. doi:10.1007/s00535-016-1242-9
38. Parada Venegas D, De la Fuente MK, Landskron G, et al. Short Chain Fatty Acids (SCFAs)-mediated gut epithelial and immune regulation and its relevance for inflammatory bowel diseases. *Front Immunol*. 2019;10:277. doi:10.3389/fimmu.2019.00277
39. Fukuda S, Toh H, Hase K, et al. Bifidobacteria can protect from enteropathogenic infection through production of acetate. *Nature*. 2011;469 (7331):543–547. doi:10.1038/nature09646
40. den Besten G, van Eunen K, Groen AK, Venema K, Reijngoud DJ, Bakker BM. The role of short-chain fatty acids in the interplay between diet, gut microbiota, and host energy metabolism. *J Lipid Res*. 2013;54(9):2325–2340. doi:10.1194/jlr.R036012
41. Collins J, Robinson C, Danhof H, et al. Dietary trehalose enhances virulence of epidemic Clostridium difficile. *Nature*. 2018;553(7688):291–294. doi:10.1038/nature25178

42. Masoodi M, Pearl DS, Eiden M, et al. Altered colonic mucosal Polyunsaturated Fatty Acid (PUFA) derived lipid mediators in ulcerative colitis: new insight into relationship with disease activity and pathophysiology. *PLoS One*. 2013;8(10):e76532. doi:10.1371/journal.pone.0076532
43. Schniers A, Goll R, Pasing Y, Sørbye SW, Florholmen J, Hansen T. Ulcerative colitis: functional analysis of the in-depth proteome. *Clin Proteomics*. 2019;16:4. doi:10.1186/s12014-019-9224-6
44. Bryan PF, Karla C, Edgar Alejandro MT, Sara Elva EP, Gemma F, Luz C. Sphingolipids as mediators in the crosstalk between microbiota and intestinal cells: implications for inflammatory bowel disease. *Mediators Inflamm*. 2016;2016:9890141. doi:10.1155/2016/9890141
45. Sewell GW, Hannun YA, Han X, et al. Lipidomic profiling in Crohn's disease: abnormalities in phosphatidylinositols, with preservation of ceramide, phosphatidylcholine and phosphatidylserine composition. *Int J Biochem Cell Biol*. 2012;44(11):1839–1846. doi:10.1016/j.biocel.2012.06.016
46. McNeil NI, Cummings JH, James WP. Short chain fatty acid absorption by the human large intestine. *Gut*. 1978;19(9):819–822. doi:10.1136/gut.19.9.819
47. Topping DL, Clifton PM. Short-chain fatty acids and human colonic function: roles of resistant starch and nonstarch polysaccharides. *Physiol Rev*. 2001;81(3):1031–1064. doi:10.1152/physrev.2001.81.3.1031
48. Huda-Faujan N, Abdulamir AS, Fatimah AB, et al. The impact of the level of the intestinal short chain Fatty acids in inflammatory bowel disease patients versus healthy subjects. *Open Biochem J*. 2010;4:53–58. doi:10.2174/1874091X01004010053
49. Machiels K, Joossens M, Sabino J, et al. A decrease of the butyrate-producing species Roseburia hominis and Faecalibacterium prausnitzii defines dysbiosis in patients with ulcerative colitis. *Gut*. 2014;63(8):1275–1283. doi:10.1136/gutjnl-2013-304833
50. Idle JR, Gonzalez FJ. Metabolomics. *Cell Metab*. 2007;6(5):348–351. doi:10.1016/j.cmet.2007.10.005
51. Shenghua L, Xin W, Huixia S, Hui Z, Bingbing L. Improvement in the analytical capabilities of LA-ICP-MS for high spatial resolution U-Pb dating of zircon using mixed-gas plasma. *J Anal Methods Chem*. 2020;2020:1819639. doi:10.1155/2020/1819639
52. Want EJ. LC-MS Untargeted Analysis. *Methods Mol Biol*. 2018;1738:99–116.
53. Johnson CH, Ivanisevic J, Siuzdak G. Metabolomics: beyond biomarkers and towards mechanisms. *Nat Rev Mol Cell Biol*. 2016;17(7):451–459. doi:10.1038/nrm.2016.25
54. Liao Z, Zhang S, Liu W, et al. LC-MS-based metabolomics analysis of Berberine treatment in ulcerative colitis rats. *J Chromatogr B Analyt Technol Biomed Life Sci*. 2019;1133:121848. doi:10.1016/j.jchromb.2019.121848
55. Zou J, Shen Y, Chen M, et al. Lizhong decoction ameliorates ulcerative colitis in mice via modulating gut microbiota and its metabolites. *Appl Microbiol Biotechnol*. 2020;104(13):5999–6012. doi:10.1007/s00253-020-10665-1
56. Yuan Z, Yang L, Zhang X, Ji P, Hua Y, Wei Y. Mechanism of Huang-lian-Jie-du decoction and its effective fraction in alleviating acute ulcerative colitis in mice: regulating arachidonic acid metabolism and glycerophospholipid metabolism. *J Ethnopharmacol*. 2020;259:112872. doi:10.1016/j.jep.2020.112872
57. Huang JH, Huang XH, Chen ZY, Zheng QS. Sun RY Equivalent dose conversion between animals and between animals and humans in pharmacological tests. *Chin J Clin Pharm Therap*. 2004;9:1069–1072.
58. Cui L, Guan X, Ding W, et al. Scutellaria baicalensis Georgi polysaccharide ameliorates DSS-induced ulcerative colitis by improving intestinal barrier function and modulating gut microbiota. *Int J Biol Macromol*. 2021;166:1035–1045. doi:10.1016/j.ijbiomac.2020.10.259
59. Wu ZC, Zhao ZL, Deng JP, Huang JT, Wang YF, Wang ZP. Sanhuang Shu'ai decoction alleviates DSS-induced ulcerative colitis via regulation of gut microbiota, inflammatory mediators and cytokines. *Biomed Pharmacother*. 2020;125:109934. doi:10.1016/j.biopha.2020.109934
60. Stephens RH, Tanianis-Hughes J, Higgs NB, Humphrey M, Warhurst G. Region-dependent modulation of intestinal permeability by drug efflux transporters: in vitro studies in mdr1a(-/-) mouse intestine. *J Pharmacol Exp Ther*. 2002;303(3):1095–1101. doi:10.1124/jpet.102.041236
61. Klompus M, Ho W, Sharkey KA, McKay DM. Antisecretory effects of neuropeptide Y in the mouse colon are region-specific and are lost in DSS-induced colitis. *Regul Pept*. 2010;165(2–3):138–145. doi:10.1016/j.regpep.2010.05.014
62. Asad S, Wegler C, Ahl D, et al. Proteomics-informed identification of luminal targets for in situ diagnosis of inflammatory bowel disease. *J Pharm Sci*. 2021;110(1):239–250. doi:10.1016/j.xphs.2020.11.001
63. Pang Z, Chong J, Zhou G, et al. MetaboAnalyst 5.0: narrowing the gap between raw spectra and functional insights. *Nucleic Acids Res*. 2021;49(W1):W388–W396. doi:10.1093/nar/gkab382
64. Han Q, Li H, Jia M, et al. Age-related changes in metabolites in young donor livers and old recipient sera after liver transplantation from young to old rats. *Aging Cell*. 2021;20(7):e13425. doi:10.1111/acel.13425
65. Wang X, Saud SM, Wang F, et al. Protective effect of ShaoYao decoction on colitis-associated colorectal cancer by inducing Nrf2 signaling pathway. *J Ethnopharmacol*. 2020;252:112600. doi:10.1016/j.jep.2020.112600
66. Wang X, Saud SM, Zhang X, Li W, Hua B. Protective effect of Shaoyao Decoction against colorectal cancer via the Keap1-Nrf2-ARE signaling pathway. *J Ethnopharmacol*. 2019;241:111981. doi:10.1016/j.jep.2019.111981
67. Hong ZC, Cai Q, Duan XY, et al. Effect of compound Sophorae decoction in the treatment of ulcerative colitis by tissue extract metabolomics approach. *J Tradit Chin Med*. 2021;41(3):414–423. doi:10.19852/j.cnki.jtcm.2021.03.009
68. Sturm A, Zeeh J, Sudermann T, Rath H, Gerken G, Dignass AU. Lisofylline and lysophospholipids ameliorate experimental colitis in rats. *Digestion*. 2002;66(1):23–29. doi:10.1159/000064418
69. Zou D, Pei J, Lan J, et al. A SNP of bacterial blc disturbs gut lysophospholipid homeostasis and induces inflammation through epithelial barrier disruption. *EBioMedicine*. 2020;52:102652. doi:10.1016/j.ebiom.2020.102652
70. Zhai L, Huang T, Xiao HT, et al. Berberine suppresses colonic inflammation in dextran sulfate sodium-induced murine colitis through inhibition of cytosolic phospholipase A2 activity. *Front Pharmacol*. 2020;11:576496. doi:10.3389/fphar.2020.576496
71. Schneider H, Braun A, Füllekrug J, Stremmel W, Ehehalt R. Lipid based therapy for ulcerative colitis-modulation of intestinal mucus membrane phospholipids as a tool to influence inflammation. *Int J Mol Sci*. 2010;11(10):4149–4164. doi:10.3390/ijms11104149
72. Olofsson KE, Andersson L, Nilsson J, Björkbacka H. Nanomolar concentrations of lysophosphatidylcholine recruit monocytes and induce pro-inflammatory cytokine production in macrophages. *Biochem Biophys Res Commun*. 2008;370(2):348–352. doi:10.1016/j.bbrc.2008.03.087
73. Qin X, Qiu C, Zhao L. Lysophosphatidylcholine perpetuates macrophage polarization toward classically activated phenotype in inflammation. *Cell Immunol*. 2014;289(1–2):185–190. doi:10.1016/j.cellimm.2014.04.010
74. Sawai T, Drongowski RA, Lampman RW, Coran AG, Harmon CM. The effect of phospholipids and fatty acids on tight-junction permeability and bacterial translocation. *Pediatr Surg Int*. 2001;17(4):269–274. doi:10.1007/s003830100592

75. Ehehalt R, Wagenblast J, Erben G, et al. Phosphatidylcholine and lysophosphatidylcholine in intestinal mucus of ulcerative colitis patients. A quantitative approach by nanoElectrospray-tandem mass spectrometry. *Scand J Gastroenterol*. 2004;39(8):737–742. doi:10.1080/00365520410006233
76. Franzosa EA, Sirota-Madi A, Avila-Pacheco J, et al. Gut microbiome structure and metabolic activity in inflammatory bowel disease. *Nat Microbiol*. 2019;4(2):293–305. doi:10.1038/s41564-018-0306-4
77. Zhang X, Choi FF, Zhou Y, et al. Metabolite profiling of plasma and urine from rats with TNBS-induced acute colitis using UPLC-ESI-QTOF-MS-based metabonomics--a pilot study. *FEBS J*. 2012;279(13):2322–2338. doi:10.1111/j.1742-4658.2012.08612.x
78. Wang R, Gu X, Dai W, et al. A lipidomics investigation into the intervention of celastrol in experimental colitis. *Mol Biosyst*. 2016;12(5):1436–1444. doi:10.1039/C5MB00864F
79. Chatterjee S, Mishra S, Suzuki SK. New vis-Tas in lactosylceramide research. *Adv Exp Med Biol*. 2015;842:127–138.
80. Chiricozzi E, Aureli M, Mauri L, et al. Glycosphingolipids. *Adv Exp Med Biol*. 2021;1325:61–102.
81. Chatterjee S, Pandey A. The Yin and Yang of lactosylceramide metabolism: implications in cell function. *Biochim Biophys Acta*. 2008;1780(3):370–382. doi:10.1016/j.bbagen.2007.08.010
82. Chatterjee S, Balram A, Li W. Convergence: lactosylceramide-centric signaling pathways induce inflammation, oxidative stress, and other phenotypic outcomes. *Int J Mol Sci*. 2021;22(4):1816. doi:10.3390/ijms22041816
83. Filimoniuk A, Blachnio-Zabielska A, Imierska M, Lebensztejn DM, Daniluk U. Sphingolipid analysis indicate lactosylceramide as a potential biomarker of inflammatory bowel disease in children. *Biomolecules*. 2020;10(7):1083. doi:10.3390/biom10071083
84. Daniluk U, Daniluk J, Kucharski R, et al. Untargeted metabolomics and inflammatory markers profiling in children with crohn's disease and ulcerative colitis-a preliminary study. *Inflamm Bowel Dis*. 2019;25(7):1120–1128. doi:10.1093/ibd/izy402
85. Bazarganipour S, Hausmann J, Oertel S, et al. The lipid status in patients with ulcerative colitis: sphingolipids are disease-dependent regulated. *J Clin Med*. 2019;8(7):971. doi:10.3390/jcm8070971
86. Haas TA, Bertomeu MC, Bastida E, Buchanan MR. Cyclic AMP regulation of endothelial cell triacylglycerol turnover, 13-hydroxyoctadecadienoic acid (13-HODE) synthesis and endothelial cell thrombogenicity. *Biochim Biophys Acta*. 1990;1051(2):174–178. doi:10.1016/0167-4889(90)90190-O
87. Engels F, van Houwelingen AH, Buckley TL, van de Velde MJ, Henricks PA, Nijkamp FP. Airway hyperresponsiveness induced by 13-hydroxyoctadecadienoic acid (13-HODE) is mediated by sensory neuropeptides. *Adv Prostaglandin Thromboxane Leukot Res*. 1995;23:361–363.
88. Henricks PA, Engles F, van Esch B, Van der linde HJ, Oosthuizen MJ, Nijkamp FP. Epithelium-derived linoleic acid metabolites modulate airway smooth muscle function. *Agents Actions Suppl*. 1990;31:283–286. doi:10.1007/978-3-0348-7379-6_39
89. Huang YW, Echeveste CE, Oshima K, et al. Anti-colonic inflammation by black raspberries through regulating toll-like receptor-4 signaling in interlukin-10 knockout mice. *J Cancer Prev*. 2020;25(2):119–125. doi:10.15430/JCP.2020.25.2.119
90. Nagata S, Suzuki J, Segawa K, Fujii T. Exposure of phosphatidylserine on the cell surface. *Cell Death Differ*. 2016;23(6):952–961. doi:10.1038/cdd.2016.7
91. He Z, Si Y, Jiang T, et al. Phosphotidylserine exposure and neutrophil extracellular traps enhance procoagulant activity in patients with inflammatory bowel disease. *Thromb Haemost*. 2016;115(4):738–751. doi:10.1160/TH15-09-0710
92. Iwatani S, Iijima H, Otake Y, et al. Novel mass spectrometry-based comprehensive lipidomic analysis of plasma from patients with inflammatory bowel disease. *J Gastroenterol Hepatol*. 2020;35(8):1355–1364. doi:10.1111/jgh.15067
93. Snodgrass RG, Huang S, Namgaladze D, et al. Docosahexaenoic acid and palmitic acid reciprocally modulate monocyte activation in part through endoplasmic reticulum stress. *J Nutr Biochem*. 2016;32:39–45. doi:10.1016/j.jnutbio.2016.01.010
94. Nicholas DA, Zhang K, Hung C, et al. Palmitic acid is a toll-like receptor 4 ligand that induces human dendritic cell secretion of IL-1β. *PLoS One*. 2017;12(5):e0176793. doi:10.1371/journal.pone.0176793
95. Ghezzal S, Postal BG, Quevrain E, et al. Palmitic acid damages gut epithelium integrity and initiates inflammatory cytokine production. *Biochim Biophys Acta Mol Cell Biol Lipids*. 2020;1865(2):158530. doi:10.1016/j.bbalip.2019.158530
96. Song J, Li J, Mourot JM, Evers BM, Chung DH. Diacylglycerol kinase regulation of protein kinase D during oxidative stress-induced intestinal cell injury. *Biochem Biophys Res Commun*. 2008;375(2):200–204. doi:10.1016/j.bbrc.2008.07.155
97. Murase T, Aoki M, Wakisaka T, Hase T, Tokimitsu I. Anti-obesity effect of dietary diacylglycerol in C57BL/6J mice: dietary diacylglycerol stimulates intestinal lipid metabolism. *J Lipid Res*. 2002;43(8):1312–1319. doi:10.1194/jlr.M200094-JLR200
98. Jangi S, Holmer AK, Dulai PS, et al. Spatial evolution of histologic and endoscopic healing in the left and right colon in patients with ulcerative colitis. *Clin Gastroenterol Hepatol*. 2022;20(4):e750–e760. doi:10.1016/j.cgh.2021.02.007